ÉCOLE CENTRALE DE NANTES SECOND YEAR OF MASTER

MASTER ARIA ROBA

2017 / 2018

Master Thesis Report

Presented by

Guillaume JEANNEAU

On 31/01/2018

Modelling and optimisation of an underactuated gripper for high-speed grasping of objects

Jury

President:	KERMORGANT Olivier	Assistant Professor at ECN, Researcher at LS2N
Evaluators:	WENGER Philippe	CNRS Director of Research at LS2N
Supervisor(s):	BRIOT Sébastien	CNRS Researcher at LS2N
	BÉGOC Vincent	Researcher, ICAM

Laboratory: Laboratoire des Sciences du Numérique de Nantes LS2N

Abstract

The hand or gripper allows robots to interact with their environment. The hands or grippers are designed such as they can grasp or manipulate an object. The grasping task requires less abilities than manipulation does. Grippers were designed because they enable us to grasp objects in a simpler way. Underactuation was moreover introduced to further simplify the command and to reduce the number of actuators. The study of their static stability was tackled. Their design process was developed, taking into account the static equations of mechanics in order to be stable and apply regular and high forces. The dynamics of the gripper and of the object begins to be studied.

In past research, the object was supposed to evolve in a two dimensional space, the objective of this master thesis is to optimally design a gripper in a dynamic approach for the grasp of 3D moving object. It has been chosen to suppose the object has a negligible displacement. New criteria are defined to check this assumption. Then the existing criteria of stability and the new criteria are analysed.

The influence of specific parameters on different criteria of stability or on objective function are analysed. It appears some parameters have a negligible effect on the static behaviour and important one on the dynamics. The opposite is true too. A new design methodology of an underactuated gripper taking into the dynamic and contact equations and taking into account the object possible movement is proposed.

Acknowledgements

In this section, I would like to thank all the persons who helped me in any way during this year, but too in all past years of study.

The first persons I want to acknowledge are my supervisors Sébastien Briot and Vincent Bégoc. Sébastien Briot manage to guide me when scientific difficulties where appearing. Vincent Bégoc helped me to understand how the project had to be carried out, and helped how to simplify a problem which at first sight is very complex and seems impossible to simplify. Moreover they were able to encourage me during this semester. They both left me organise my research all along the semester, leading to a very good work experience. I would like moreover to thank my professors during the first semester in the Master ARIA ROBA. This master of high level was very interesting. I could discover robotics, and research. I could even progress on personal skills, exchange with the promotion. I thank everybody in the team ARMEN of LS2N. The work atmosphere is great and the exchanges of knowledge helped the semester to be enriching. The exchange of cultural differences was moreover fascinating.

Beside, I thank my family, for their unbreakable encouragement and support throughout my study. Last but not least, I thank all my friend, from the one who were always here from the beginning to all the new friends I met during this year, making this year unforgettable.

Notations

α_k, β_k Ratios of lengths to compute the geometric model

$\boldsymbol{\omega}_a = \dot{\boldsymbol{\theta}}_a$ Time derivative of $\boldsymbol{\theta}_a$

$\boldsymbol{\tau}$ Total torque vector associated to angles $\mathbf{q}_a$

$\boldsymbol{\tau}_B$ Torque vector associated to angles $\boldsymbol{\theta}_a$

$\boldsymbol{\tau}_a$ open loop torque exerted on proximal links

$\boldsymbol{\tau}_d$ open loop torque exerted on distal links

$\boldsymbol{\tau}_{gi}$ Torque due to the gravity

$\boldsymbol{\theta} = \begin{bmatrix} \theta_1 & \theta_1 \end{bmatrix}^T$ Vector of phalanges angle

$\boldsymbol{\theta}_a = \begin{bmatrix} -q_{11} & q_{22} \end{bmatrix}^T$ Generalised coordinates usually chosen for the static analysis of gripper;

ΔE_p Variation of potential energy of the cylinder

Δx_G Variation of position of the cylinder center of mass

δ the penetration depth

$\dot{\delta}$ Penetration depth velocity

$\dot{\delta}^+$ Penetration depth velocity after impact

$\dot{\delta}^-$ Penetration depth velocity before impact

$\Gamma = \pm 1$ Variable defining the configuration of the hand given the angles $\mathbf{q}_a$

$\mathbf{A}$, $\mathbf{B}$, $\mathbf{J}_t$, $\mathbf{J}_{ta}$, $\mathbf{J}_{td}$ Matrices specific to the kinematics of the finger

$\mathbf{A}_s$ Matrix expressing the contact conditions for the system composed of the finger and the object

$\mathbf{b}_c$, $\mathbf{d}_c$ Vectors expressing non linear terms of accelerations

$\mathbf{c}$ Vector of Coriolis and centrifugal effect

$\mathbf{c}_t$ Vector of Coriolis and centrifugal effect for the open loop finger

$\mathbf{F}^{hand} = \begin{bmatrix} F_x & F_y \end{bmatrix}^T$ Vector of forces applied by the object on the hand

$\mathbf{J}_X$ Jacobian matrix for the end effector

$\mathbf{K}$ Matrix expressing the condition of non back-drive ability

$\mathbf{M}$ Inertia matrix of the finger

$\mathbf{M}_c$ Matrix for the expression of the form closure criteria

$\mathbf{M}_s$ Inertia matrix of the system composed of the finger and the object

$\mathbf{P}$ Projection matrix

$\mathbf{q}_a = \begin{bmatrix} q_{11} & q_{21} \end{bmatrix}^T$ Generalised coordinates defining the angle between the finger global frame and the first leg of the five bar mechanism

$\mathbf{q}_a^s$ Vector of generalised coordinates for the system composed of the finger and the object

$\mathbf{q}_a^{cyl}$ Vector of generalised coordinates for the object

$\mathbf{q}_d = \begin{bmatrix} q_{12} & q_{22} \end{bmatrix}^T$ Passive joint angle;

$\mathbf{S}$ Sorting Matrix

$\mathbf{S}_c$ Impact matrix

$\mathbf{S}_s$ Selection Matrix for the contact

$\mathbf{V}_{slip}$ Relative tangential velocity

$\mathbf{X}$ Position vector of point $O_{13} = O_{23}$

$\mathbf{x}$ Axis defined as the directions given by the line going through the point O_{21} of both finger

$\mathbf{x}_c$ Axis of the cylinder

$\mathbf{x}_{ij}$ Vector defining the principal direction of link ij

$\mathbf{y}$ Axis normal to the palm

$\mathbf{y}_{ci}$ Normal vector for phalanx i

$\mathbf{z}$ Axis normal to the hand

μ_d Dynamic coefficient of friction between the object and the hand

μ_g the dynamic coefficient of friction between the object and the ground

μ_p the static coefficient of friction between the object and the palm

μ_s Static coefficient of friction between the object and the hand

$\overrightarrow{\mathbf{AB}}$ Vector going from point A to B

ψ Angle between the principal direction of link 22 and the distal phalanx;

ρ_c Density of the cylinder

ρ_f Density of the finger

τ Torque exerted by the motor

τ_{c_i} Torque due to contact forces

τ_{fric} Frictional torque of an object rotating on the top of an other one

τ_{s22} Torque exerted by the spring on point O_{22}

$\theta_1 = q_{21}$ the angle of the proximal phalanx

θ_2 the angle of the distal phalanx

θ_c Angle with axis $\mathbf{z}$ of the cylinder

$\tilde{F}$ Mean force of applied forces

b Length of the palm

e Restitution coefficient

E_{cyl} Energy given to the cylinder after impact

F_n^{Ground} and $\mathbf{F}_t^{Ground}$ Normal force norm and tangential force exerted by the object on the ground

F_n^{Palm} and $\mathbf{F}_t^{Palm}$ Normal force norm and tangential force exerted by the object on the palm

F_t^{Palm} tangential force norm exerted by the object on the palm

G Object center of mass

g Gravity constant

h_2 Constructed length of the finger

h_c Height at which the cylinder is grasped

K Contact stiffness

k_c Distance from the center of gravity to the point of contact projected on the axes

k_{ci} Contact length for the object in contact with phalanx i

k_i Contact length for phalanx i

L_c Length of the cylinder

l_{hand} Length of the hand

l_{ij} Length of link ij

m Number of grasped object

m_c Mass of the cylinder

m_f Equivalent mass of the finger for the contact with proximal phalanx

m_{cyl} Equivalent mass of the cylinder for the contact

N_{ci} Projected point P_{ci}

N_i Projected point P_i

O Reference point of the frame attached to the hand, placed at the center of the palm;

$O_{13} = O_{23}$ End effector point at the intersection of link 12 and 22

O_{ij} Point at the basis of link ij, $i, j \in (1, 2)$

p Ratio of length l_{21} and l_{11}

P_{ci} Contact point on the object in contact with phalanx i

P_i Contact point on the phalanx i in contact with the object

r Transmission ratio

R_c Radius of the cylinder

S_{ij} Point at the center of mass of link ij

t_{22} Length of distal phalanx

v_d Dynamic transition velocities of the continuous friction force

v_s Static transition velocities of the continuous friction force

w Finger phalanges and links radius

W_{fric} Work of friction

$x_{S_{ij}}$ X-coordinates of the position of point S_{ij}

$y_{S_{ij}}$ Y-coordinates of the position of point S_{ij}

zz_{ij} Inertia of link ij at its origin

${}^j\mathbf{f}_n = \begin{pmatrix} {}^j f_1 & {}^j f_2 \end{pmatrix}^T$ Vector of normal forces applied by respectively the proximal and distal phalanges. The index $j \in (1, 2)$ is the number of the finger, it can be omitted.

${}^j\mathbf{F}_i$ Total force expressed in global frame and in 3D of phalanx i and finger j

${}^j\mathbf{F}_{ni}$ Normal force expressed in global frame and in 3D of phalanx i and finger j

${}^j\mathbf{F}_{ti}$ Tangential force expressed in global frame and in 3D of phalanx i and finger j

${}^j\mathbf{J}$ Jacobian matrix specific to the contact. The index $j \in (1, 2)$ is the number of the finger, it can be omitted.

${}^j\mathbf{J}_n$ and ${}^j\mathbf{J}_t$ Jacobian matrices for normal and tangential velocity between the finger and the object

${}^j\mathbf{T}$ Transmission matrix linking $\boldsymbol{\omega}_a$ to $\dot{\boldsymbol{\theta}}_a$. The index $j \in (1, 2)$ is the number of the finger, it can be omitted.

List of Figures

List of Tables

Introduction

General objective

In industry or in domestic application, different objects have to be moved from one place to another. Depending on the task to perform, the object can be taken by different system. Two tasks are generally distinguished: grasping and manipulation. The suction cup for example can give the possibility to grasp an object with a flat surface. Inspired by human hand, many fully actuated hands were designed too. They have the ability to grasp or to manipulate. But knowing that two or three fingers can perform a grasp, the gripper was invented. The gripper is a system able to grasp and hold an object with many possible designs. Fully actuated hands and grippers enable the grasping and manipulation of complex objects, with different shapes, structures, volumes or weights. The hand complexity has then increased a lot over time. The control is consequently very complex and the cost is increased. This complexity is not always necessary. A good simple design can lead to a good adaptability too. A more recent solution is under-actuated grippers. They have the advantage both to have a reduced number of actuators and the ability to adapt their shape to the object to grasp.

In this study, a typical task has been chosen. The gripper could be used in a domestic application. The objective of the gripper is to grasp a bottle of water laid on a table. The bottle could have different shape, different masses depending on how full it is for example. The suction cup is not suitable because of the unknown surface. Moreover a complete hand is more complex and therefore to expensive for this seemingly simple task. The objective is then to optimally design an under-actuated gripper to grasp a typical bottle of water. It has been chosen a bottle of one litter. To do the study, the bottle was approximated by a cylinder of diameter $8cm$, a height of $20cm$ and a mass of $1kg$. Different size and masses will then be tested to check the adaptability of the gripper

Several challenges have been found in the past for the design of under-actuated gripper. The first challenge is to know if the grasping of the object is successful. A grasp is successful if the object remains in the gripper during the grasping process and once the gripper is closed, even if perturbations appear in its environment. To define this condition scientifically, several conditions of stability have been defined in the past. In particular, the criteria of form closure, force positiveness or palm force positiveness have been used in [2]. The form-closure criteria has then been extended to underactuated hands in [3]. This criteria means that geometrically speaking all possible movements of the object are prevented. Then, as the form closure can be very restricitive, the force closure criteria defined and used in [1] gives the ability to know if the object's movement is prevented due to applied forces on the object. The problem of those two criteria is that their output are valid once the gripper is closed but not while the gripper is closing.

When we talk about performance of a gripper, we could simply think about the time performances of the gripper. The previously defined criteria are necessary conditions but do not contain any idea of time in it. That is why, in recent studies some techniques are used to go step by step to a design stable during the grasping process. In [4], the gripper has an adjustable compliance, leading to an adaptation of properties to the gripping phases. This way the forces exerted on the object can be low during the graping, and make the hand really adaptable. Once the gripping phase is finished, the configuration is changed and the forces applied are higher, giving the ability to hold the object well. The problem is that no index of stability is defined for the dynamic phase, meaning that no validation is possible for the grasping phase. In [5], the dynamics of the gripper are taken into account to ensure that all the phalanx touch the object at the same time. The problem is that the dynamic of the object is not taken into account and may result in instability if the object changes. The dynamics of the object are not yet taken into account. Then, in [6], the object dynamic is taken into account in a plane. Three degree of freedom are then given to the object. The optimal design of the gripper is then done to catch this moving object. The problem of this study is that the object is not supposed as being a 3D object. That is why, in this document the object could theoretically move in the complete space. The bottle can fall because a moment is exerted on the bottle through the gripper and the ground. It can also slip on the floor. Two new criteria will then been defined to ensure that the object won't move too much during the grasping process. We will link those criteria to the physical property of the object. Moreover, it will possible to say at which speed or with which torque applied, the grasping can be done. As a result the modelling and design analysis of an under-actuated gripper for high-speed grasping of objects has been carried out.

Gripper design

The selected general topology of the gripper is based on a five bar linkage mechanism. The theory in static and dynamic of the five bar linkage has been already carefully studied in [7]. The methodology and general idea of design presented in this report can be extended to other types of transmission like pulley and cable. The general idea of this design is the following one. You can refer to figure 1. The actuation is done on link (11). This action is transmitted to the distal phalanx (22) through a transmission bar (12). A spring between the proximal (21) and distal phalanx (22) prevent the distal phalanx to fold before that the proximal one does. The spring transmit then the energy of the motor to the proximal phalanx (21). A contact between the distal and proximal phalanx stop the opening of the finger. This way, when no effort but that of the spring are applied on the finger, the finger is fully open. This is the configuration shown on figure 1. When no contact with the object occurs, the complete finger is closing. When contact with the proximal phalanx occurs, the distal phalanx can fold, forcing the spring to stretch.

General Analysis Methodology

The gripper design has to take several aspect of mechanics into account. The first step will be to do a review of existing design requirement. Moreover the literature on contact modelling has been studied to model later the behaviour of both the object and the gripper. The kinematic model, the static model and the dynamic model are presented. From those model, condition of successful grasp are presented. In particular, the kinematic conditions are defined to prevent any singularities. The definition of the static conditions of stability are applied according to existing literature. Finally new conditions for the dynamic stability are defined. To be more

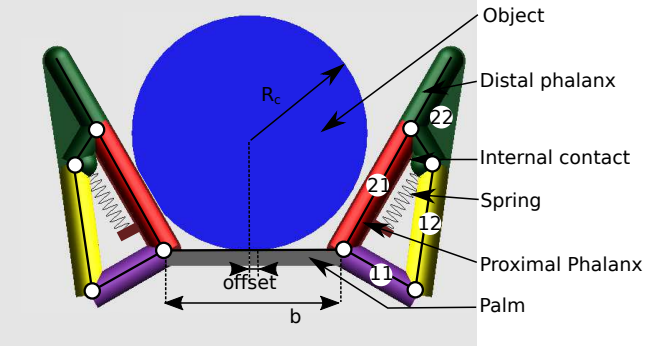

Figure 1: Presentation of the hand

precise, it is checked that the object doesn't move after forces and impact are applied. By following those three steps, the influence of design parameters on the performances. The effect of each of the parameters on the different physical phenomena is studied. From those results, a new design methodology is proposed. This methodology will lead to a robust design, crossing no singularity, which can perform the form closure, applying maximum forces in static and assure that object does not move. The all design is moreover created such as it can close quickly.

Chapter 1

State of the art

The analysis of the state of the art has been carried out in order to know what is already existing and know what are the limits of existing works. In this first part, some of the existing design methodology for gripper are explained. The objective in this part will be to see the limits of existing theory. Moreover existing work which has been used along the thesis, either in order to design or model the gripper. Two different areas had to be join in this mater thesis, the theory of gripper, their static and dynamic model, their design methodology and stability criteria. The second area related to the design of gripper according to their dynamic is the problematic of contact.

1.1 Existing gripper and criteria : Going to a dynamic design

In this first section, a rapid analysis of static criteria of stability which can be used in the design of gripper is done. Then the existing criteria for the design taking into account the dynamics are presented.

1.1.1 Static design

The first idea for the design of under-actuated gripper is that it is not that easy to hold an object. As degree of freedom exist in the gripper due to under-actuation, if the gripper is not well design, the object could be removed of the gripper even if the static equilibrium is reached. That was the first big issue in the design of gripper.

Instability phenomenon of under-actuated mechanism

Before explaining how the design of gripper can be designed, it must be understood what type of instability phenomena could appear. How is it possible that an object can move even if the gripper seems to envelop the object?

Instability phenomenon of under-actuated mechanism The first part of the answer is given in [2]. This study is still today a principal reference for the analysis of under-actuated hand. Here after are defined some phenomena leading to instability or necessary conditions for different stability. Indeed, depending on the criteria of stability, some design could be stable for some of the criteria, and not for other.

Avoiding the roll back phenomenon The roll back phenomenon or ejection phenomenon presented in [2] is the phenomenon by which the finger will close on itself, slipping on the object. It has been firstly explained in the publication [8]. To prevent this phenomenon, the first advise is to add some limits to the dimension of the gripper. This way, the finger will adapt reasonably on the profile contour of the object to catch. For example, if the number of phalanges is increased, the risk of this phenomenon to appear increases considerably and is moreover much harder to predict. This phenomenon is an unstable phenomenon of underactuated gripper.

Force positiveness and palm force positiveness The condition of positive reaction forces given on inequality (1.1) must be fulfilled too. In particular, when applying the condition of static stability on the finger when the finger is closed, this condition must be fullfilled. Indeed if it is not fullfilled, it simmply mean that the contact cannot occur. There is not static stability. This has been expressed in [9]. It is a necessary condition to have stability of the grasp. It expresses simply that one body can not attract the other when there is a contact. This could be an hypothesis for some particular materials. In particular the suction effect could appear. But we will consider it is not the case for our system. Moreover it expresses that some of the forces can be null. In that case, there is loss of contact or it simply express that the object does not touch the phalanx.

$$\mathbf{f}_n \geq \mathbf{0} \tag{1.1}$$

With:

- $\mathbf{f}_n$ the vector of normal components of the forces applied by phalanges.

If this condition is not respected, it means that the hypothesis of contacts are not valid. There is the loss of one contact. The roll-back phenomenon could be appearing in this case.

Similarly, after applying the static equilibrium on the object to grasp, the resultant force on the palm must be positive. If not, it means that the object will go away of the grasp. There is no static stability.

Absence of form closure The first criteria is the form closure property. Firstly adapted to a non underactuated gripper, this property has been generalised to all type of gripper in [10]. The definition given is the following one:

> *"A grasp is said to be form-closed if, and only if, for any variation of the configuration of the grasp at least one of the unilateral kinematic constraints is violated."*

If this condition is not verified, it means that the object can move if external perturbation appears, even if the gripper and object are in a stable configuration. The form closure property is checked when three conditions are verified. They are listed bellow :

- There is no penetration between the object and the gripper;
- The mechanism is non backdriveable
- The palm is in contact with the object

This condition has been checked during our study. Detailed mathematical expression are given in 3.2.2. This condition could be to strong. Indeed, sometime, the movement of an object is possible on a geometrical point of view but impossible due to forces equilibrium. The friction in particular could give the ability to avoid any movement. That is why the following condition is defined.

Force closure The force closure is an other type of closure, less restrictive than the form closure. Two different types of force closure are presented in [1]. The active force closure and the passive force closure. The active force closure can be used for manipulation. It characterises the ability of a hand to manipulate the object in all possible directions. If an object is actively force closed, the forces applied on the object can be controlled in all possible directions. This is much more complex than passive force closure and is much more than what is needed in the gripper we want to design. The passive force closure characterises the ability of the gripper to apply reaction forces in all possible directions. Those reaction forces are not controlled in the case of passive form closure. This type of closure gives more liberty than the form closure because the friction is of great importance in the grasp. It is well known that it is easier to grasp an object with a lot of friction. The force closure will take it into account contrary to form closure.

Design rules or advises for the design of under-actuated mechanism

In this part some advise found in different publication are shown for the design of under-actuated gripper.

Form closure necessity equation The simplest design rule appears in [3]. This design rule define the necessary actuation and phalanx in order to be able to assure a form closure on the object. This condition is not sufficient to perform the form closure.

The necessary equation is presented on equation (1.2).

$$n_k \geq n_f + 1 \tag{1.2}$$

With:

- n_k is the number of one-sided constraint applied by the mechanism
- n_f is the number of degree of freedom we want to block

The quantity n_k can be calculated from the number of constraints due to contact which are unilateral n_u and from the unilateral constraint bring by unilateral mechanism with the equality given on equation (1.3).

$$n_k = n_u + n_c \tag{1.3}$$

Then it is possible to express the total number of degree of freedom which is the sum of the one from the hand n_p and the one from the object d.

$$g = n_p + d \tag{1.4}$$

Choice of the spring The spring plays an important role in the design of underactuated gripper. Some spring are absolutely necessary in the design of gripper. Indeed as the gripper studied are underactuated, it is necessary to prevent uncontrolled motion of the gripper. Their objective is to be sure of the position of the gripper when the gripper is at rest. They prevent indeed the gripper to close without actuation. Some other external or internal force can lead to incoherent motion, the inertial effect, the weight can lead to unwanted motion.

But, as presented in [9], springs will reduce the stability because they are opposed to the actuation torque. Indeed, they are opposed to the grasping direction of closure. The distal forces are reduced, the grasp is then less efficient.

Only few papers deal with the optimal placement of springs and minimise the spring stiffness. The work done in the Master thesis [11] show the importance of the placement of spring. From

this, one placement of the spring is determined. A spring constant and type of spring is moreover chosen.

It seems but appropriate to minimise the spring constant in order to prevent any unwanted closure of the mechanism. A calculation of the minimal spring constant will then be proposed in this document.

Notion of isotropic finger An isotropic finger is a finger with which all phalanx forces are equal. This condition permits to have a strong grasp. A force isotropic underactuated gripper has been designed in [12]. The gripper designed is a two fingers gripper with two phalanges each. The forces applied on proximal phalanges and distal phalanges should be as equal as possible for the sake of stability. In this publication, a variable pulley radius is used in order to make the two forces exactly equal. The stability analysis of this design has then been carried out then in [13].

But in general, the force isotropy is never achieved in most of the gripper. Moreover this condition is in general not robust to the variation of the object. This property is valid only on one precise point of contact on each phalanges and then for one particular object. That is why in some different paper, a criteria is constructed to minimize the difference between the forces, the isotropy not being obligatory reached.

Tangential and normal forces for whole hand grasping An index is presented in [2]. The axis normal to the palm is the **y** axis, the axis aligned with the palm is the **x** axis. Moreover, we assume that the object is fixed, only one finger is considered. We consider the other finger is symmetric and do then a similar work. This index assure two tasks. The first property checked is the palm form positiveness. The second task of this index is to assure that the component F_x along **x** of the resultant force should be greater that the resultant along **y**, F_y. The index is defined on equation (1.5).

$$I_{xy} = \frac{1}{m} \sum_{i=1}^{m} \frac{min(F_{x,i}, EF_{y,i})}{T_a} \delta(F_{y,i}) \tag{1.5}$$

With :

- E is the number of phalanges grasping the object
- $\delta(F_{y,i}) = \begin{cases} 1 & if \quad F_{y,i} < 0, \\ 0 & else \end{cases}$
- T_a the actuation force
- m is the number of objects

Equalisation of forces Different criteria were used for the purpose of equalizing all applied forces on the object. The publication [12] even expresses the condition to have an isotropic finger. The problem, as expressed in [2], is that we should not be confused between stability and isotropy. A finger will be stable at the precise point where the grasp is isotropic but can be unstable close to this position. It is but a good condition to have a powerful grasp. Indeed if the distal forces are big, it will help to have the palm force positiveness. Different publications uses then a criteria to improve the ratio between distal and proximal forces. This is done by trying to make them equal.

The publication [14] uses the criteria α_1 for this purpose. This criteria is function of the forces and will be null if all forces are equal.

$$\alpha_1 = \sum_{i=1}^{n} (\tilde{F} - f_i)^2 \tag{1.6}$$

With :

- $\tilde{F}$ is the mean force of all normal forces.
- f_i is the normal force applied on phalanx i.
- n is the number of phalanges of one finger.

Similarly, the publication [15] defines the criteria presented on equation (1.7). The difference here is that this criteria is defined directly for a certain number of configurations. This way several objects can be considered.

$$\beta_1 = \left(\sum_{j=1}^{N} \sum_{i=1}^{n} (f_i^j - \tilde{F}^j)^2 \right) - \tilde{F} \tag{1.7}$$

With :

- N is the number of configuration.
- n is the number of phalanges.
- f_i^j is the force exerted by the phalanx i and for the configuration j.
- $\tilde{F}$ is the mean force of all configuration and phalanges.
- $\tilde{F}^j$ is the mean force of all phalanges for the configuration j.

1.1.2 Dynamic criteria

After some criteria have been studied for static behaviour, it is possible to define some dynamic criteria. Only few criteria have been defined in the past and no general stability has been defined.

Time to stability

The time to stability could be useful in order to achieve a high speed grasping. As explained in [4], a good robustness of the grasp is a first good point for high speed motion. Indeed it can then resist to high accelerations. But it is not sufficient. The closure time of the grasp is very important to take advantage of this robustness. It is then suggested to improve the grasp speed. In [11], a time to stability is then defined. The time to stability can be defined with the following conditions.

The time to stability is the time necessary to the gripper to go from the initial state to a stable state. The stable state is defined by :

- The positiveness of the forces is checked. (See equation (1.1))
- The contact force computed must match the forces computed through the static model

Successful grasp range

The paper [6] gives a criteria that we can apply in dynamics. The successful grasp range (SGR) is defined.

$$SGR = \frac{A_{SG}}{A_{WS}} \tag{1.8}$$

With :

- A_{SG} the area on which the object can initially be placed to achieve a stable grasp.
- A_{WS} is the total workspace area that the finger can reach.

Control and Lyapunov stability

A possible largely used stability criteria which is used today in robotics is the Lyapunov stability. It has not been yet applied on underactuated gripper. The mathematical definition was found in [16]. This document was not read but seemed to be an interesting document for stability of gripper mechanism.

A point x is stable in the sense of Lyapunov if the relation given on equation (1.9) is checked.

$$\exists \delta > 0, \quad ||x(t_0)|| < \delta \Rightarrow ||x(t)|| < \epsilon, \forall t \geq t_0 \tag{1.9}$$

This stability was allude to in [2]. The case of this stability in the case of the grapstate area. They explain here that they tried to find a Lyapunov potential function. No such a function were find. The analysis of one of the grapstate area leads them to conclude that maybe no such function could be find. Nothing being sure about it.

A Lyapunov stability could be one possibility, and if possible, it would be an assurance of the dynamic stability of the gripper. It was but not found during the present study

1.2 Contact between solids

When the finger will touch the object to catch, several physical phenomena appear. If two objects have a relative velocity before they touch, an impact will occur. This impact generate a small deformation on both objects, resulting in high forces. The energy is then transmitted from one body to an other one. Elastic and plastic deformations will result in different rate of energy transfer. The influence of this contact has not yet been carefully studied for catching an object. Several phenomena are then possible. If all the contact energy is finally absorbed, the normal relative velocity between the body is null but a force still occurs due to both the normal contact and friction. This will affect the stability of the grasp too.

On this part a short review is done to remind the basic notion of contact used then to evaluate the dynamic behaviour of the finger and to check the stability conditions. The forces expression will be necessary to evaluate the dynamic behaviour of the gripper, and check that the forces won't lead to instability when the relative normal velocity between the two solids is null. The energy is necessary to evaluate the stability of the cylinder in case of impact.

1.2.1 Expression of contact forces

The study of impact energy and forces is a subject dealt with in the past. The publication [17] make a comparative analysis of existing contact model. In this part the necessary theory has been extracted.

During an impact between two objects, the transfer of energy is done by the material deformation. The material deformation can be decoupled in two different parts. There is first an elastic deformation.

The model for elastic deformation is presented in [18]. The relation is presented on equation (1.10) and is part of the Hertz contact theory.

$$F_n = K\delta^n \tag{1.10}$$

With:

- F_n is the normal contact forces applied between the two bodies.
- δ is the penetration depth.
- K the contact stiffness
- n is the penetration exponent equal to 3/2 in the elastic case.

This model becomes inaccurate when losses and a plastic behaviour appears. The publication [17] compares then the evolution of contact model and explains what are the assumptions made by each model and in which case the models are relevant.

A general form of the forces between two solids in contact is then presented on equation (1.11).

$$F_n = K\delta^{3/2} + \chi\delta^m\dot{\delta} \tag{1.11}$$

With:

- $\dot{\delta}$ is the penetration depth velocity.
- χ is the damping coefficient.
- m is the penetration exponent for the damping and is generally taken as equal to 3/2.

An other issue of the contact model is that the conservation of energy must be obtained. In particular the energy law presented in part 1.2.3 must be validated with the force given previously. This way the expression of the forces of contact is consistent with the energy of impact. In particular, the coefficient of restitution e is used. It is defined in function of the velocity before impact $\dot{\delta}^-$ and the velocity after impact $\dot{\delta}^+$ on the following equation .

$$e = \frac{\dot{\delta}^+}{\dot{\delta}^-} \tag{1.12}$$

The model selected leads to the contact normal force F_n expressed on equation (1.13).

$$F_n = K\delta^{3/2}\left(1 + \frac{8}{5}\frac{(1-e)}{e}\frac{\dot{\delta}}{\dot{\delta}^-}\right) \tag{1.13}$$

This model was selected because it has the advantage to work both for high or low coefficient of restitution.

1.2.2 Friction model

When normal forces are computed, it is possible then to have the expression of the tangential forces and frictional torques.

Model of Coulomb

A model possible to have the tangential forces is the model of Coulomb. Two different cases appear in the model of Coulomb. It depends on the ratio of normal forces F_n and tangential forces $\mathbf{F}_t$ norm. The tangential forces can be in a plane if we consider a three dimensional contact. If it is inferior to a threshold named static coefficient μ_s as shown on equation (1.14), the relative velocity between the two bodies at the point of contact is null.

$$\|\mathbf{F}_t\| \leq \mu_s |F_n| \tag{1.14}$$

In that case, the static equations should give both normal forces and tangential forces because two geometric constraints appears in the two main directions of the contact.

If the inequality (1.14) is not checked, a relative velocity $\mathbf{v}$ will appear between the two considered bodies. In that case, a new coefficient named kinetic friction coefficient μ_k defines the ratio between the two forces as shown on equation (1.15). The tangential forces $\mathbf{F}_t$ are opposed to the relative velocity v between the two bodies at the point of contact.

$$\mathbf{F}_t = -\mu_s |F_n| \frac{\mathbf{V}_{slip}}{\left\|\mathbf{V}_{slip}\right\|} \tag{1.15}$$

Some other models exists and are presented in [7]. In particular, we often take a viscous friction model in addition. In this case, the friction force is proportional to the speed. In a joint, moreover the Stribeck phenomenon can appear. It correspond to a diminution of the friction coefficient at a low relative speed before the proportional behaviour. It is due to the lubrication. In our case, the relative velocity between the two bodies is not high enough to see this phenomenon appearing, the simple model of Coulomb will be sufficient.

Expression of frictional torques

It is possible too that a relative rotational velocity appears between two bodies. This can be seen as if infinitesimal tangential friction appears all around the center of the zone of contact. By integration over the main direction, we obtain the tangential forces F_t, and by calculating the moment of friction at the center by integration, we obtain the moment of friction. This moment depends on the position considered for the contact. In the plane where contact occurs, we can consider two points O and A. The frictional moment on O, $\mathbf{M_O}$, can be expressed by the following relation:

$$\mathbf{M_O} = \mathbf{M_A} + \overrightarrow{OA} \times \mathbf{F_t} \tag{1.16}$$

The frictional moment at the center of the contact with a circular contact can be approximated by a relation which link it to the normal force applied. This relation presented on equation (1.17) is the equation of an ellipse. This equation is valid only at the onset of sliding.

$$\left(\frac{F_t}{\mu_s (F_n)_{max}}\right)^2 + \left(\frac{\tau_{fric}}{(\tau_{fric})_{max}}\right)^2 = 1 \tag{1.17}$$

With:

- F_t the frictional force resultant.
- μ_s the friction coefficient.
- $(F_n)_{max}$ is the maximum normal force applied.
- τ_{fric} is the frictional moment.

- $(\tau_{fric})_{max}$ is the maximum frictional moment. It can be expressed with the relation presented on equation (1.18).

$$(\tau_{fric})_{max} = \int_A \mu |r| \, C_k \frac{N}{\pi a^2} \left[1 - \left(\frac{r}{a} \right)^k \right]^{\frac{1}{k}} dA \tag{1.18}$$

With:

- a the radius of contact area.
- r the radius in the surface for integration calculation.
- A the area of contact.
- C_k a coefficient depending on the pressure distribution chosen (1.5 for circular distribution, 1 for uniform distribution).

As this moment will be exerted on the direction normal to the finger phalanges $\mathbf{y}_{2i}$ if the axe of the cylinder $\mathbf{x}_c$ is aligned with the normal of the finger plane $\mathbf{z}$.

1.2.3 Impact energy and energy transfer

Energy transfer for two balls

The energy loss between two bodies resulting from the impact during the total contact time is called the impact energy. This energy loss will result in the loss of kinetic energy in the total system composed of the two objects in contact. The result is known for two balls and is presented on equation (1.19). The publication [19] express the kinematic of contact.

$$\Delta E = m_{tot} V_{impact}^2 (1 - e^2) \tag{1.19}$$

With :

- $V_{impact} = V_2^- - V_1^-$ the impact velocity.
- e the coefficient of restitution.
- $m_{tot} = \frac{m_1 m_2}{m_1 + m_2}$ the equivalent mass of the system in contact.

We can notice here the use of the coefficient of restitution. This coefficient of restitution is defined as the ratio between the relative velocity before and the one after the impact. This coefficient is equal to one when all the energy is conserved in the system, all the kinetic energy at the moment of impact becomes a potential energy in the material, through elasticity. If this coefficient is equal to zero, all the energy is converted to heat through plastic loss in the material.

It is moreover possible to express the velocity of each of the ball in reference to the velocity before the impact using the relations shown on equation (1.20) and (1.21).

$$V_1^+ = m_{tot} \left(\left(\frac{1}{m_2} - \frac{e}{m_1} \right) V_1^- + \frac{1+e}{m_1} V_2^- \right) \tag{1.20}$$

$$V_2^+ = m_{tot} \left(\left(\frac{1}{m_1} - \frac{e}{m_2} \right) V_2^- + \frac{1+e}{m_2} V_1^- \right) \tag{1.21}$$

Energy transfer during an impact for a multi body system

The theory has then been extended to system of body. This theory is important for the underactuated gripper, because it gives the velocity of both the impacting leg and of the distal one when only one occurs. The system composed of the object and one finger has 5 degree of freedom instantaneously at the moment of impact. There is only one actuator, this system becomes highly underactuated. The publication [20] give the possibility to apprehend the dynamic of such a system during an impact. The relation expressed on equation (1.22) gives the generalised coordinates velocity of the complete system after the impact in function of the velocity before the impact.

$$\dot{\mathbf{q}}^{+} = \dot{\mathbf{q}}^{-} - (e+1)\mathbf{S}_c\dot{\mathbf{q}}^{-} + (\mathbf{I} - \mathbf{S}_c)\mathbf{M}^{-1}\mathbf{i}_\tau \tag{1.22}$$

With :

- $\mathbf{i}_\tau = \int_0^{\delta_t} \boldsymbol{\tau} dt$ the other forces during the impact period;
- $\mathbf{q}$ the generalised coordinates of the system;
- $\mathbf{I}$ the identity matrix;
- $\mathbf{M}$ the inertia matrix;
- $\mathbf{S}_c$ constructed from the contact closure equations and from the inertia matrix;
- e the restitution coefficient.

This relation will be then adapted to create a new criteria of stability in part 3.3.1.

Chapter 2

Model

The model of the system will be used to compute the dynamic behaviour of the hand. First, the geometric and kinematic model of the hand is presented. Then the static model leading to the dynamic model are given. The object dynamics can be modelled too. The dynamic model of the object was first used to understand the behaviour of the system. Understanding that the study could focus on the condition on which the object would move, it was not useful too evaluate the cylinder dynamics precisely. Only the notations and parameter specific to the cylinder are here presented. The dynamic model of the object can be found on appendix A. Then starting from the geometry of contact going to the kinematics of contact, it will be possible to present the model of contact.

2.1 Geometric and kinematic model of the finger

To begin with, it is necessary to present the geometric model of the system. On figure 2.1 is presented the parameters specific to the hand.

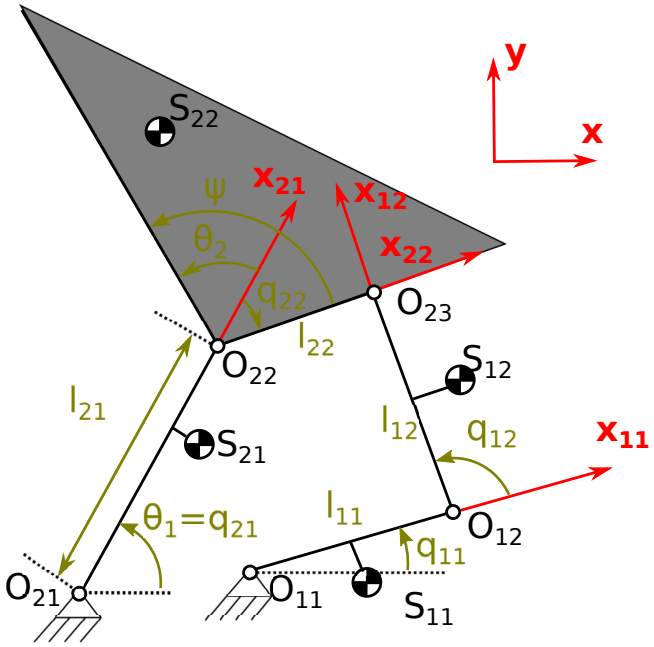

Figure 2.1: Parameter used in this section

2.1.1 Geometric model

In this part, the objective is to define the existing relation relations due to the geometry of the finger. Before going in detail, the angles and vector of the finger are define as follow. $\mathbf{x}_{ij}$ are the vector going from the point O_{ij} to O_{ij+1}. The angles q_{i1} are defined as the angle between axes $\mathbf{x}$ and $\mathbf{x}_{i1}$. The angles q_{i2} are defined as the angle between axes $\mathbf{x}_{i1}$ and $\mathbf{x}_{i2}$.

Direct geometric model

The direct geometric model is the model giving the ability to compute the position of point O_{13} which is noted $\mathbf{X}$. Starting from the Chasles relation (2.1), we can evaluate the position of the points O_{i2}.

$$\overrightarrow{\mathbf{OO}_{i2}} = l_{i1}\mathbf{x}_{i1} + \overrightarrow{\mathbf{OO}_{i1}} \tag{2.1}$$

With :

- $\mathbf{x}_{i1} = \begin{pmatrix}\cos(q_{i1}) & \sin(q_{i1})\end{pmatrix}^T$ the 2D vector defining the principal direction of link $i1$;
- l_{i1} the length of link $i1$;
- $\overrightarrow{\mathbf{OO}_{i1}}$ a constant vector defining the position of the finger basis.

From those relation, it is possible to define two ratios α_k and β_k using equations (2.2) to (2.4).

$$r_i = \frac{l_{i2}}{\left\|\overrightarrow{\mathbf{O}_{22}\mathbf{O}_{12}}\right\|} \tag{2.2}$$

$$\alpha_k = \frac{1}{2}(1 - r_1^2 + r_2^2) \tag{2.3}$$

$$\beta_k = \sqrt{r_2^2 - \alpha_k^2} \tag{2.4}$$

The ratio r_i express the ratio of the length of the distal link over the distance going from O_{22} to O_{12}. α_k is the ratio of the distance between the point O_{23} and its projection on $\overrightarrow{\mathbf{O}_{22}\mathbf{O}_{12}}$ over the length $\left\|\overrightarrow{\mathbf{O}_{22}\mathbf{O}_{12}}\right\|$. β_k is the ratio of the distance between the point O_{22} and the projection of O_{23} on $\overrightarrow{\mathbf{O}_{22}\mathbf{O}_{12}}$ over the length $\left\|\overrightarrow{\mathbf{O}_{22}\mathbf{O}_{12}}\right\|$. A solution to the direct geometric model exist if $|r_2| > |\alpha_k|$. This means that with the angle given, the finger must be mountable, with length sufficiently long enough.

Once defined, two solutions equations exist for the direct geometric model, the equation (2.5) give them in function of the parameter $\Gamma = \pm 1$.

$$\mathbf{X} = \overrightarrow{\mathbf{OO}_{22}} + \alpha_k\overrightarrow{\mathbf{O}_{22}\mathbf{O}_{12}} + \Gamma\beta_k\mathbf{E}\overrightarrow{\mathbf{O}_{22}\mathbf{O}_{12}} \tag{2.5}$$

Passive leg angle

Once the active angle are calculated, the passive angle are computed. The equation (2.6) give them.

$$q_{2i} = -q_{1i} + \tan^{-1}\left(\overrightarrow{\mathbf{O}_{i1}\mathbf{O}_{13}} \cdot \mathbf{y} - l_{i1}\sin(q_{1i}), \overrightarrow{\mathbf{O}_{i1}\mathbf{O}_{13}} \cdot \mathbf{x} - l_{i1}\cos(q_{1i})\right) \tag{2.6}$$

The last passive angle on joint positioned on point O_{13} is calculated by the following relation.

$$q_{13} = q_{21} + q_{22} - q_{11} - q_{12} \tag{2.7}$$

We can define here the angle vector $\boldsymbol{\theta} = \begin{bmatrix}\theta_1 & \theta_2\end{bmatrix}^T$ containing the angle $\theta_1 = q_{21}$ and $\theta_2 = q_{22} + \psi$. Those angles are the angle specific to the contact and to the static model. The generalised coordinates vector $\mathbf{q}_a = \begin{bmatrix}q_{11} & q_{21}\end{bmatrix}^T$ and the passive angle $\mathbf{q}_d = \begin{bmatrix}q_{12} & q_{22}\end{bmatrix}^T$ are the angles specific to the dynamic model.

2.1.2 Kinematic model of the finger

The kinematic model is used to compute all joints velocity. In particular, we will be able to get the generalised coordinates by integration of the acceleration. Then the passive leg velocity must be computed, this is done using the direct kinematic model and with the passive leg kinematics. The obtained matrix will then be useful in the dynamic model of the robot.

Direct kinematic model

The direct kinematic model is formalised under the form presented on equation (2.8).

$$\begin{aligned}\dot{\mathbf{X}} &= -\mathbf{A}^{-1}\mathbf{B}\dot{\mathbf{q}}_a \\ &= \mathbf{J}_X\dot{\mathbf{q}}_a\end{aligned} \tag{2.8}$$

With the matrix $\mathbf{A}$ and $\mathbf{B}$ defined on equation (2.9) and (2.10).

$$\mathbf{A} = \begin{pmatrix}\cos(q_{11}+q_{12}) & \sin(q_{11}+q_{12}) \\ \cos(q_{21}+q_{22}) & \sin(q_{21}+q_{22})\end{pmatrix} \tag{2.9}$$

$$\mathbf{B} = -\begin{pmatrix}l_{11}\sin(q_{12}) & 0 \\ 0 & l_{21}\sin(q_{22})\end{pmatrix} \tag{2.10}$$

In order to avoid any loss of degree of freedom or loss of degree of actuation, those matrix must be invertible. The singularities are presented in section 3.1.

Expression of passive joint velocity

Using the velocity of the point O_{13}, the passive joint velocity can be obtained under the form presented on equation (2.11).

$$\dot{\mathbf{q}}_d = \mathbf{J}_{td}^{-1}\left(\mathbf{J}_t\dot{\mathbf{X}} - \mathbf{J}_{ta}\dot{\mathbf{q}}_a\right) \tag{2.11}$$

$$\mathbf{J}_{td} = \begin{pmatrix}l_{12} & 0 \\ 0 & l_{22}\end{pmatrix} \tag{2.12}$$

$$\mathbf{J}_t = \begin{pmatrix}-\sin(q_{11}+q_{12}) & \cos(q_{11}+q_{12}) \\ -\sin(q_{21}+q_{22}) & \cos(q_{21}+q_{22})\end{pmatrix} \tag{2.13}$$

$$\mathbf{J}_{ta} = \begin{pmatrix}l_{12}+l_{11}\cos(q_{12}) & 0 \\ 0 & l_{22}+l_{21}\cos(q_{22})\end{pmatrix} \tag{2.14}$$

2.1.3 Kinematic model order 2

The kinematic model at this level is not directly used. Indeed the computation of the acceleration of the passive legs is not necessary. Those relations are but a primary condition to be able to compute the dynamic model. The dynamic model will then use the following defined matrices.

Direct kinematic model order 2

The first step is to compute the acceleration of point O_{13}. It can be obtained under the form presented on equation (2.15) by derivative of equation (2.8).

$$\ddot{\mathbf{X}} = -\mathbf{A}^{-1}(\mathbf{B}\ddot{\mathbf{q}}_a + \mathbf{b}_c) \tag{2.15}$$

The term $\mathbf{b}_c$ presented on equation (2.16) is a term which will be used in the dynamic model.

$$\mathbf{b}_c = \dot{\mathbf{A}}\dot{\mathbf{X}} + \dot{\mathbf{B}}\dot{\mathbf{q}}_a \tag{2.16}$$

With the derivative of matrix $\mathbf{A}$ and $\mathbf{B}$ given on equation (2.17) and (2.18).

$$\dot{\mathbf{A}} = \begin{pmatrix} -(\dot{q}_{11}+\dot{q}_{12})\sin(q_{11}+q_{12}) & (\dot{q}_{11}+\dot{q}_{12})\cos(q_{11}+q_{12}) \\ -(\dot{q}_{21}+\dot{q}_{22})\sin(q_{21}+q_{22}) & (\dot{q}_{21}+\dot{q}_{22})\cos(q_{21}+q_{22}) \end{pmatrix} \tag{2.17}$$

$$\dot{\mathbf{B}} = -\begin{pmatrix} l_{11}\dot{q}_{12}\cos(q_{12}) & 0 \\ 0 & l_{21}\dot{q}_{22}\cos(q_{22}) \end{pmatrix} \tag{2.18}$$

Expression of passive joint second order velocity

[2] Similarly, we can express the passive joint acceleration from equation (2.11). It is given on equation (2.19).

$$\ddot{\mathbf{q}}_d = \mathbf{J}_{td}^{-1}\left(\mathbf{J}_t\ddot{\mathbf{X}} - \mathbf{J}_{ta}\ddot{\mathbf{q}}_a + \mathbf{d}_c\right) \tag{2.19}$$

The variable $\mathbf{d}_c$ is computed using equation (2.20) to (2.22).

$$\mathbf{d}_c = \dot{\mathbf{J}}_t\dot{\mathbf{X}} - \dot{\mathbf{J}}_{ta}\dot{\mathbf{q}}_a \tag{2.20}$$

$$\dot{\mathbf{J}}_t = \begin{pmatrix} (\dot{q}_{11}+\dot{q}_{12})\cos(q_{11}+q_{12}) & (\dot{q}_{11}+\dot{q}_{12})\sin(q_{11}+q_{12}) \\ (\dot{q}_{21}+\dot{q}_{22})\cos(q_{21}+q_{22}) & (\dot{q}_{21}+\dot{q}_{22})\sin(q_{21}+q_{22}) \end{pmatrix} \tag{2.21}$$

$$\dot{\mathbf{J}}_{ta} = -\begin{pmatrix} l_{11}\dot{q}_{12}\sin(q_{12}) & 0 \\ 0 & l_{21}\dot{q}_{22}\sin(q_{22}) \end{pmatrix} \tag{2.22}$$

2.2 Static model

The static model is first derived from the theory first presented in [9] and then generalized in [2]. This theory is used in particular to check the force closure and the palm force positiveness. I then changed the choice of coordinates to do the parallel between this theory and the theory presented in [7]. This way the dynamic results will be related to the static results.

2.2.1 First approach based on the theory of Birglen

A first approach is used to evaluate the static equilibrium of a finger. This first methodology is used in particular to check further if the condition of static stability are met. In particular the conditions of form closure, palm force positiveness or force positiveness can be checked with this model. This model has been developped in [2]. We will see in this section the existing theory and the a relation with the kinematics presented in [7]. The model is presented with two phalanges. Moreover we assume that beside the contact forces only two torques are applied, the torque applied on the finger τ and the one applied by the spring τ_s.

Internal equilibrium

The static equilibrium can be written under the form presented on equation (2.23).

$$ {}^{i}\boldsymbol{\tau}_B^{T\,i}\mathbf{T}^{-1} = {}^{i}\mathbf{f}_n^{T\,i}\mathbf{J} \tag{2.23} $$

With :

- $\boldsymbol{\tau_B} = \begin{bmatrix} -\tau_m & \tau_s \end{bmatrix}^T$ being the 2D vector of torques applied on rotational joint, respectively present on point O_{11} and O_{22};
- $\mathbf{T}$ the transmission matrix;
- $\mathbf{J}$ the Jacobian matrix;
- $\mathbf{f}_n$ the normal force applied on each phalanx.
- i the index corresponding to the finger 1 or 2.

It can be shown, by guessing that no torque are transmitted through the point of contact, that the Jacobian matrix can be written under the form presented on equation (2.24).

$$ {}^{i}\mathbf{J} = {}^{i}\mathbf{J}_n + \mu_s {}^{i}\mathbf{J}_t \tag{2.24} $$

The matrix ${}^{i}\mathbf{J}_n$ and ${}^{i}\mathbf{J}_t$ are the Jacobian matrix relating the joint velocity $\dot{\boldsymbol{\theta}}$, respectively, to the normal and tangential velocity at the point of contact. This relation is valid for both the fingers i. μ_s is the static coefficient of friction between the object and the gripper.

The matrix ${}^{1}\mathbf{J}_n$ and ${}^{1}\mathbf{J}_t$ are expressed under the form presented on equation (2.25) and (2.26).

$$ {}^{1}\mathbf{J}_n = \begin{pmatrix} k_1 & 0 \\ \mathbf{r}_{12}^T\mathbf{x}_2 & k_2 \end{pmatrix} \tag{2.25} $$

$$ {}^{1}\mathbf{J}_t = \begin{pmatrix} 0 & 0 \\ \mathbf{r}_{12}^T\mathbf{y}_2 & 0 \end{pmatrix} \tag{2.26} $$

The transformation matrix is the matrix linking the angular velocity at the level of actuated joints $\boldsymbol{\omega}_a = \begin{bmatrix} -\dot{q}_{11} & \dot{q}_{22} \end{bmatrix}^T$ to the angular velocity of link in contact with the object. $\dot{\boldsymbol{\theta}} = \begin{bmatrix} \dot{\theta}_1 & \dot{\theta}_2 \end{bmatrix}^T$ as shown on equation (2.27).

$$ \dot{\boldsymbol{\theta}} = {}^{i}\mathbf{T}\boldsymbol{\omega}_a \tag{2.27} $$

The transformation matrix can then be expressed under the form presented in [9] and shown on equation (2.28).

$$ {}^{i}\mathbf{T} = \begin{pmatrix} 1 & -\frac{h_2}{h_2+l_{21}} \\ 0 & 1 \end{pmatrix} \tag{2.28} $$

In this relation ${}^{i}\mathbf{T}$ is the transformation matrix of finger i, h_2 is the distance between O_{21} and the intersection of $(O_{21}O_{22})$ and $(O_{12}O_{23})$.

This transformation matrix can then be expressed using the kinematic matrix linking the passive joint $\dot{\mathbf{q}}_d$ to the active joints $\dot{\mathbf{q}}_a$. This equation is obtained using equation (2.8) and (2.11).

$$ \begin{aligned} \dot{\mathbf{q}}_p &= \mathbf{J}_{td}^{-1} \left(\mathbf{J}_t \mathbf{J}_X - \mathbf{J}_{ta} \right) \dot{\mathbf{q}}_a && (2.29) \\ &= \mathbf{J}_d \dot{\mathbf{q}}_a && (2.30) \\ &= \begin{pmatrix} J_d^{11} & J_d^{12} \\ J_d^{21} & J_d^{22} \end{pmatrix} \dot{\mathbf{q}}_a && (2.31) \end{aligned} $$

This definition of matrix $\mathbf{J}_d$ give the possibility to deal with the case where points O_{11} and point O_{21} are not coincident. This way we can express the matrix ${}^{i}\mathbf{T}$ under the following form :

$$ {}^{i}\mathbf{T} = \begin{pmatrix} -\frac{J_d^{21}}{J_d^{22}} & -\frac{1}{J_d^{22}} \\ 0 & 1 \end{pmatrix} \tag{2.32} $$

In the case points O_{11} and point O_{21} are coincident, the matrix $\mathbf{J}_d$ is not invertible any more and we have $\frac{J_d^{21}}{J_d^{22}} = -1$. The form presented on equation (2.28) is obtained.

Expression of the reprojection Matrix

From this model we managed to obtain the normal forces from the torque and spring present on the gripper. For what it may concern the tangential forces, they depend on the external condition and static stability on the object must be checked. To check that the hand is able to perform this stability, a first criteria will be the palm force positiveness. The worst case happen when external forces applied on the object tends to go away from the palm. In this case, the hand is able to apply forces through normal and tangential forces. And in that case the tangential forces are directed toward the palm and have for maximum magnitude $\mathbf{f}_t = \mu \mathbf{f}_n$.

With the given model, it is no possible to obtain the wrench applied on the object. This is done by projection of the forces in the 2D global frame by using the matrix called the projection matrix which is define for normal forces in [2]. By adding the tangential forces, the force is expressed using equation (2.33).

$$ \begin{aligned} \begin{pmatrix} F_x^1 \\ F_y^1 \end{pmatrix} &= {}^{1}\mathbf{P}\mathbf{f} \\ &= \begin{pmatrix} {}^{1}\mathbf{P}_n & {}^{1}\mathbf{P}_t \end{pmatrix} \begin{pmatrix} \mathbf{f}_n \\ \mathbf{f}_t \end{pmatrix} && (2.33) \\ &= \begin{pmatrix} -\sin(\theta_1) & -\sin(\theta_1+\theta_2) & -\cos(\theta_1) & -\cos(\theta_1+\theta_2) \\ \cos(\theta_1) & \cos(\theta_1+\theta_2) & -\sin(\theta_1) & -\sin(\theta_1+\theta_2) \end{pmatrix} \begin{pmatrix} \mathbf{f}_n \\ \mathbf{f}_t \end{pmatrix} \end{aligned} $$

With :

- ${}^1\mathbf{P}$ the projection matrix;
- ${}^1\mathbf{P}_n$ the projection matrix relative to normal forces;
- ${}^1\mathbf{P}_n$ the projection matrix relative to tangential forces.

We have to be careful here that the relations presented in this section are valid for the case where the contact occurs with the right finger noted 1 when z axis is toward us and palm is toward positive y. The forces exerted by the second finger have to be derived similarly, in particular the matrix $\mathbf{J}$ and $\mathbf{P}$ and $\mathbf{P_t}$ must be slightly modified.

Finally the force applied by the different phalanges is expressed on equation (2.34). This force is expressed in the plane of the hand.

$$\mathbf{F}^{hand} = \begin{pmatrix} F_x \\ F_y \end{pmatrix} = \begin{pmatrix} F_x^1 \\ F_y^1 \end{pmatrix} + \begin{pmatrix} F_x^2 \\ F_y^2 \end{pmatrix} \tag{2.34}$$

2.2.2 Second approach : generalisation for dynamics

The approach becomes slightly different to evaluate the dynamic behaviour of the system. This approach is based on the theory explained in [7]. With this approach, all the efforts are dealt with such as they are not correlated to the choice of coordinates. This gives the ability to take any efforts in the simulation. In particular the gravity can be added. This theory will first give the possibility to extend the model to a dynamic model. Moreover we will see in part 4.1.1 that the theory can be used to choose a spring.

To begin with, the theory uses the previously defined generalised coordinates q_a. They can be called active coordinates even if no forces are applied. Then the three joints remaining joints are called passive angle and noted q_p. The methodology for this method is to virtually open the loop of the gripper, express the forces applied in this case and close then the loop by using the kinematics equation and theory of Lagrange. Only the results are detailed further.

External forces applied on the proximal and distal phalanx

The first step is then to evaluate the torque applied on active joints by opening the loop. The expression can be seen on equation (2.35).

$$\boldsymbol{\tau}_a = -\boldsymbol{\tau}_{g_1} - \boldsymbol{\tau}_{g_2} + \begin{pmatrix} 0 \\ \tau_{c_1} + \tau_{c_2} \end{pmatrix} + \begin{pmatrix} \tau & 0 \end{pmatrix} \tag{2.35}$$

Similarly the passive joint torque are expressed on equation (2.36).

$$\boldsymbol{\tau}_d = -\boldsymbol{\tau}_{g_2} + \begin{pmatrix} 0 \\ \tau_{s22} \end{pmatrix} + \begin{pmatrix} 0 \\ \tau_{c_2} \end{pmatrix} \tag{2.36}$$

With :

- $\boldsymbol{\tau}_{g_i}$ are the equivalent torque applied by gravity.
- τ_{c_i} are the torque due to contact forces
- τ_{s22} is the torque applied by the spring

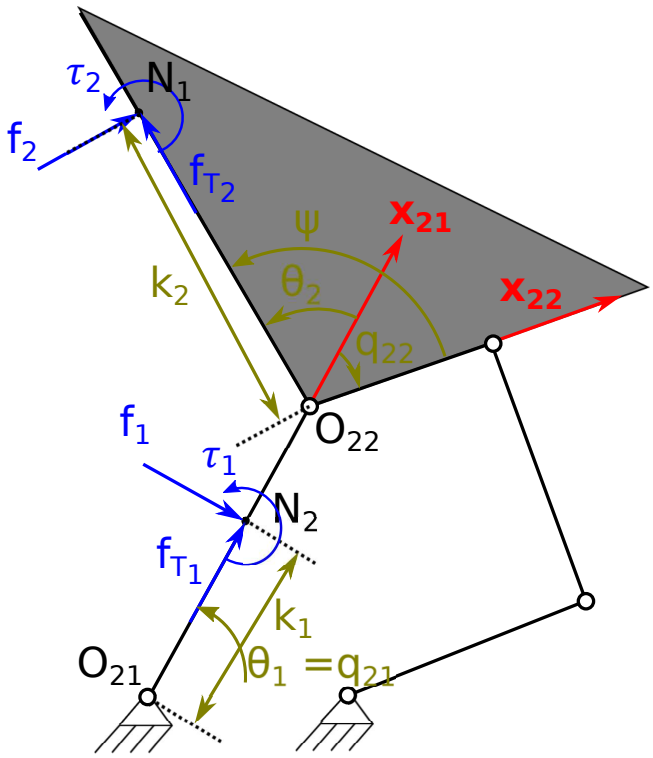

Figure 2.2: Expression of Contact Torque from Forces

Expression of contact torque

The expression of contact equivalent torque is done using the figure 2.2. The Jacobian matrix found on equation (2.24) could be found from here.

$$\tau_{c_1} = \left(\overrightarrow{\mathbf{O_{21}N_1}} \times \mathbf{F}_1 + \overrightarrow{\mathbf{O_{21}O_{22}}} \times \mathbf{F}_2\right) \cdot \mathbf{z} \tag{2.37}$$

$$= -k_1 f_1 - l_{21}\left(f_2 \cos(\theta_2) + f_{t2} \sin(\theta_2)\right) \tag{2.38}$$

$$\tau_{c_2} = \left(\overrightarrow{\mathbf{O_{22}N_2}} \times \mathbf{F}_2\right) \cdot \mathbf{z} \tag{2.39}$$

$$= -k_2 f_2 \tag{2.40}$$

With :

- k_i the height of contact for phalanx i
- $\mathbf{f}_n = \begin{pmatrix} f_1 & f_2 \end{pmatrix}^T$ the normal forces.
- $\mathbf{f}_t = \begin{pmatrix} f_{t1} & f_{t2} \end{pmatrix}^T$ the tangential forces.

Loop closure and static equation

After applying the loop closure with all the torques previously defined, we obtain the total torque equivalent torque $\boldsymbol{\tau}$ applied on the active joints under the form presented on equation (2.41).

$$\boldsymbol{\tau} = \boldsymbol{\tau}_a + \mathbf{J}_d^T \boldsymbol{\tau}_d \tag{2.41}$$

The equation corresponding then to the static equilibrium is simply $\boldsymbol{\tau} = \mathbf{0}$.

2.3 Dynamic model

The dynamic model of one of the finger is presented in this section. This dynamic model was based on the theory given in [7]. This model is used to be able to simulate the finger. The direct dynamic model express the joint coordinate accelerations in function of all external force applied on the finger. Once the accelerations are obtained, the in integration of accelerations and a solver will lead to the time evolution of the finger. This is the only way to be able to compute all forces along the time and to compute the time of closure of the finger.

2.3.1 Gravity expression for the finger

The gravity is expressed in any configuration of the finger toward the ground reference. The use of to variable, g_{eq} which is the equivalent gravity field and θ_g are used for that. If the gravity is normal to the plane of finger, g_{eq} is equal to 0. If it is not, the angle θ_g is the angle between $\mathbf{x}$ and the projected vector of gravity $\mathbf{g}_eq = \mathbf{g} - (\mathbf{g} \cdot \mathbf{z})\mathbf{z}$. The projection of the gravity field on the plane of the finger will give $g_{eq} = norm\mathbf{g}_eq$.

Then the components of the torque applied on the finger is obtained on the two following equations.

$$\tau_{i1}^g = g_{eq}\left((m_{i1}x_{Si1} + m_{i2}l_{i1})\sin(q_{i1} - \theta_g) + m_{i1}y_{Si1}\cos(q_{i1} - \theta_g)\right) \tag{2.42}$$

$$\tau_{i2}^g = g_{eq}\left((m_{i2}x_{Si1})\sin(q_{i1} + q_{i2} - \theta_g) + m_{i2}y_{Si2}\cos(q_{i1} + q_{i2} - \theta_g)\right) \tag{2.43}$$

The torque vector corresponding to proximal or distal forces is then expressed.

$$\boldsymbol{\tau}_{g1} = \begin{pmatrix} \tau_{11} & \tau_{21} \end{pmatrix}^T \tag{2.44}$$

$$\boldsymbol{\tau}_{g2} = \begin{pmatrix} \tau_{12} & \tau_{22} \end{pmatrix}^T \tag{2.45}$$

2.3.2 Direct Dynamic Model

The dynamic model gives then the generalised coordinates acceleration in function of the previously defined torque.

$$\ddot{\mathbf{q}}_a = \mathbf{M}^{-1}(\boldsymbol{\tau} - \mathbf{c}) \tag{2.46}$$

With :

- $\mathbf{M}$ the inertia matrix;
- $\mathbf{c}$ the matrix of Coriolis and centrifugal effects.

The Inertia matrix is expressed using equation (2.47) to (2.50).

$$\mathbf{M} = \begin{pmatrix} \mathbf{I}_2 & \mathbf{J}_d \end{pmatrix} \mathbf{S}^T \begin{pmatrix} \mathbf{M}_{t1} & \mathbf{0}_2 \\ \mathbf{0}_2 & \mathbf{M}_{t2} \end{pmatrix} \mathbf{S} \begin{pmatrix} \mathbf{I}_2 \\ \mathbf{J_d} \end{pmatrix} \tag{2.47}$$

$$\mathbf{M}_t = \begin{pmatrix} \mathbf{M}_{t1} & \mathbf{0}_2 \\ \mathbf{0}_2 & \mathbf{M}_{t2} \end{pmatrix} \tag{2.48}$$

$$\mathbf{M}_{t1} = \begin{pmatrix} zz_{i1} + zz_{i2} + m_{i2}l_{i1}^2 + 2zz_i^1 & zz_{i2} + zz_i^1 \\ zz_{i2} + zz_i^1 & zz_{i2} \end{pmatrix} \tag{2.49}$$

$$\mathbf{zz}_i = \begin{pmatrix} zz_i^1 \\ zz_i^2 \end{pmatrix} m_{i2} l_{i1} \mathbf{R}_{q_{i2}} \begin{pmatrix} x_{S_{i2}} \\ y_{S_{i2}} \end{pmatrix} \tag{2.50}$$

With :

- zz_{ij} the inertia along z of the link ij and on the point O_{ij};
- l_{ij} the length of the link ij;
- m_{ij} the math of the link ij;
- $\begin{pmatrix} x_{Sij} & y_{Sij} \end{pmatrix}$ the position of the center of gravity in the frame attached to the body ij and relative to the point O_{ij};
- $\mathbf{zz}_i$ is an intermediary matrix to calculate the inertia coefficient corresponding to the bodies $i2$;
- $\mathbf{R}_{q_{i2}}$ the matrix of rotation in the plane of angle q_{21};
- $\mathbf{S} = \begin{pmatrix} 1 & 0 & 0 & 0 \\ 0 & 0 & 1 & 0 \\ 0 & 1 & 0 & 0 \\ 0 & 0 & 0 & 1 \end{pmatrix}$ is a sorting matrix.

The Coriolis and centrifugal effect matrix is then expressed using equation (2.51) to (2.55).

$$\mathbf{c} = \begin{pmatrix} \mathbf{I}_2 & \mathbf{J}_d \end{pmatrix} \mathbf{S}^T \left(\mathbf{c}_t + \mathbf{M}_t \mathbf{S} \begin{pmatrix} \mathbf{0}_{21} \\ \mathbf{J}_{td}^{-1} \mathbf{a}_d \end{pmatrix} \right) \tag{2.51}$$

$$\mathbf{c}_t = \mathbf{S} \begin{pmatrix} \mathbf{c}_{ta} \\ \mathbf{c}_{td} \end{pmatrix} \tag{2.52}$$

$$c_{ta}^i = \left(\dot{q}_{i1}^2 - \left(\dot{q}_{i1} + \dot{q}_{i2} \right)^2 \right) zz_i^2 \tag{2.53}$$

$$c_{td}^i = \dot{q}_{i1}^2 zz_i^2 \tag{2.54}$$

$$\mathbf{a}_d = \mathbf{d}_c - \mathbf{J}_t (\mathbf{A}^{-1} \mathbf{b}_c) \tag{2.55}$$

2.4 Contact model

The dynamic model being known for the finger, the forces of contact between the finger and the object must be computed. The forces of contact are dependant of the kinematic as expressed on equation (1.13) and (1.15). To be able to use those expression, the geometry and kinematic equations of contact are necessary. Once obtained, the forces can be projected onto the normal plane of the finger. The obtained forces will then be used on equation (2.38) and (2.40). In the case the object would move, the normal forces of the contact are different from the normal forces applied on the finger. The present following methodology can be applied in that case. The results are presented in both cases.

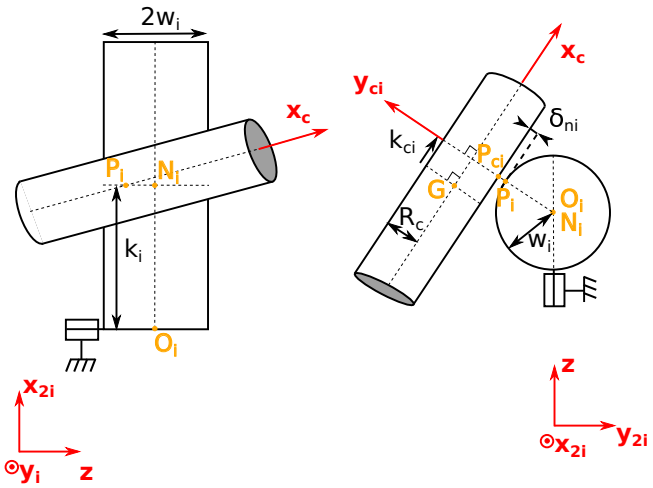

Figure 2.3: Geometry and notations of cylinder contact

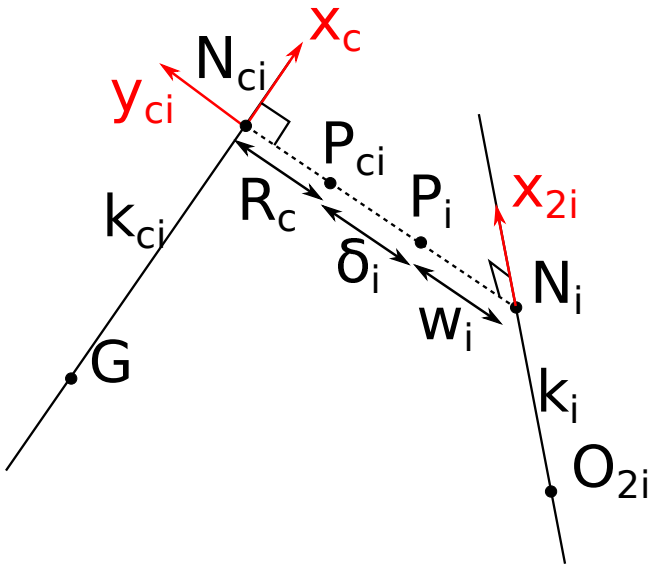

Figure 2.4: Geometry and notations of cylinder contact with two lines

2.4.1 Kinematic of two lines

The first objective is to find the penetration depth δ_i between one of the phalanx $i \in (1, 2)$ and the object. To do it a geometric analysis must be down.

The figure 2.3 presents the geometry. The point of contact of the finger is called P_i and $P_{ci}$for the cylinder. The distance δ can be defined as the distance between those two points. We define the length of contact k_i for the finger as the length of the projection $\overrightarrow{O_{2i}N_i}$ of the vector $\overrightarrow{O_{2i}P_i}$ on $\mathbf{x}_{2i}$. Similarly, k_{ci} is the length of the projection $\overrightarrow{GN_{ci}}$ of the vector $\overrightarrow{GP_{ci}}$ on the axis of the cylinder $\mathbf{x}_c$. The figure 2.4 show the problem can then be seen as the resolution of the kinematics of two lines. We can note here that the lengths k_i will influence the dynamic of the finger as shown on equation 2.38 and 2.40. Similarly, k_{ci} influence the dynamic of the object. They have to be found too.

Given the two straight lines with an origin point for each line named O_{2i} and G. They have for unitary direction vector $\mathbf{x}_{2i}$ and $\mathbf{x}_c$. It is possible to find a line orthogonal to both the lines and coincident with both the lines. This line has a unitary direction vector $\mathbf{y}_{ci}$. The relation (2.56) gives the condition to obtain this line.

$$\mathbf{x}_{2i}^T \mathbf{y}_{ci} = \mathbf{x}_c^T \mathbf{y}_{ci} = 0 \tag{2.56}$$

The points N_i and N_{ci} are the intersections points. The distances k_i and k_{ci} can be express thanks to equation (2.57).

$$\begin{pmatrix} k_i \\ k_{ci} \end{pmatrix} = \begin{bmatrix} 1 & -\mathbf{x}_{2i}^T\mathbf{x}_c \\ \mathbf{x}_{2i}^T\mathbf{x}_c & -1 \end{bmatrix}^{-1} \begin{bmatrix} \mathbf{x}_{2i}^T \\ \mathbf{x}_c^T \end{bmatrix} \overrightarrow{O_{2i}G} \tag{2.57}$$

The vector going from point N_i to N_{ci} can then be expressed with the relation (2.58).

$$\overrightarrow{\mathbf{N}_i\mathbf{N}_{ci}} = \overrightarrow{\mathbf{O}_{2i}\mathbf{G}} + k_i\mathbf{x}_{2i} - k_{ci}\mathbf{z}_c \tag{2.58}$$

The distance d_i from N_i to N_{ci} is then simply the norm of this vector, the unitary direction vector $\mathbf{y}_{ci}$ is obtained by dividing by this norm. The penetration depth is then obtained on equation (2.59).

$$\delta_i = d_i - w_i - R_c \tag{2.59}$$

2.4.2 Contact kinematic

The second steps after having the penetration depth is to compute the relative velocity between the solid in contact. The normal velocity will be used to express the normal forces, the tangential velocity determines the tangential forces.

Once the direction of contact $\mathbf{y}_{ci}$ and the lengths k_i have been computed, it is possible to express the relative velocity between the contacting points. All the kinematic relations have been derived in three dimensions. The hypothesis being first that the cylinder could move. By definition the contact velocity is the relative velocity of the two closest points. The first point is noted P_{ci}. It is on the surface of the cylinder and belongs to the line of contact $\mathcal{L}_c$. The second point P_i belongs to the surface of the phalanx and to $\mathcal{L}_c$. The geometric position of those two points are given by equation (2.60) for the point P_{ci}, by equation (2.61) if the contact is between the proximal phalanx and the object and by equation (2.62) if the contact is done on the distal phalanx, before the tip.

$$\overrightarrow{\mathbf{G}\mathbf{P}_{ci}} = k_{ci}\mathbf{x_c} - R_c\mathbf{y}_{ci} \tag{2.60}$$

$$\overrightarrow{\mathbf{O}_{21}\mathbf{P}_1} = k_1\mathbf{x}_{21} + w\mathbf{y}_{ci} \tag{2.61}$$

$$\overrightarrow{\mathbf{O}_{21}\mathbf{P}_2} = k_2\mathbf{x}_{22} + l_{21}\mathbf{x}_{21} + w\mathbf{y}_{ci} \tag{2.62}$$

The relative velocity between the two points is then expressed by the difference between the velocity of each points, belonging to the common line $\mathcal{L}_c$ in reference to the ground as expressed on equation (2.63).

$$\mathbf{V}_{rel} = \mathbf{V}_{P_{ci}}(\mathcal{L}_c/0) - \mathbf{V}_{P_i}(\mathcal{L}_c/0) \tag{2.63}$$

After some computation, it is possible to express it, respectively on equation (2.64) and (2.65) for the proximal and distal contact. We can note that all vector are expressed in the same referential frame.

$$\mathbf{V}_{rel} = \dot{\mathbf{X}}_G + k_c\dot{\mathbf{x}}_c - k_1\dot{\mathbf{x}}_{21} - R_c\boldsymbol{\omega}_c \times \mathbf{y}_{ci} - w\dot{\theta}_1\mathbf{z} \times \mathbf{y}_{ci} \tag{2.64}$$

$$\mathbf{V}_{rel} = \dot{\mathbf{X}}_G + k_c\dot{\mathbf{x}}_c - k_2\dot{\mathbf{x}}_{22} - l_{21}\dot{\mathbf{x}}_{21} - R_c\boldsymbol{\omega}_c \times \mathbf{y}_{ci} - w(\dot{\theta}_1 + \dot{\theta}_2)\mathbf{z} \times \mathbf{y}_{ci} \tag{2.65}$$

By taking as an assumption that the cylinder is fixed, the equations become :

$$\mathbf{V}_{rel} = -k_1\dot{\mathbf{x}}_{21} - w\dot{\theta}_1\mathbf{z} \times \mathbf{y}_{ci} \tag{2.66}$$

$$\mathbf{V}_{rel} = -k_2\dot{\mathbf{x}}_{22} - l_{21}\dot{\mathbf{x}}_{21} - w(\dot{\theta}_1 + \dot{\theta}_2)\mathbf{z} \times \mathbf{y}_{ci} \tag{2.67}$$

The projection along $\mathbf{y}_{ci}$, as shown on equation (2.68) give then the penetration velocity which will be useful to compute the normal force between the two solids

$$\mathbf{V}_{rel}^{T}\mathbf{y}_{ci} = \dot{\delta} \tag{2.68}$$

The sleeping velocity given on equation (2.69) is obtained by removing the projection along $\mathbf{y}_{ci}$. This expression can be used to compute the frictional forces when the relative velocity norm is different from zero.

$$\mathbf{V}_{slip} = \mathbf{V}_{rel} - \dot{\delta}\mathbf{y}_{ci} \tag{2.69}$$

2.4.3 Contact forces expression

The previous parameters are used to express the forces exerted between the two bodies.

The normal forces are expressed using the force computed thanks to equation (1.13) with the equation (2.70).

$$\mathbf{F}_i = F_n(\delta_i, \dot{\delta}_i, \dot{\delta}_i^{-})\mathbf{y}_{ci} \tag{2.70}$$

The velocity of impact $\dot{\delta}_0$ is determined by detecting the transition between the situation where no impact occurs ($\delta < 0$) to the case where a penetration occurs ($\delta > 0$).

The frictional forces are then computed when a contact occurs during the simulation. Those forces are computed such as there is a continuity of forces. This is done using the relation given on equation (2.71)

$${}^{j}\mathbf{F}_{ti} = \mu(v_{slip})\left\|{}^{j}\mathbf{F}_{ni}\right\| \frac{\mathbf{V}_{slip}}{v_{slip}} \tag{2.71}$$

With :

- $v_{slip} = \left\|\mathbf{V}_{slip}\right\|$
- μ is a step function function of v_{slip}. It is null when v_{slip} is null and get done to $-\mu_s$ when $v_{slip} = v_s$ and raise to $-\mu_d$ when $v_{slip} > v_d$.

Those forces can be added and projected on axis $\mathbf{x}_{2i}$ and $\mathbf{y}_{2i}$ to obtain respectively the tangential f_{ti} and normal forces f_i applied on the finger. In the case neither the cylinder nor the hand origin are moving, those forces are the same as F_i and F_{ti}.

2.4.4 Force expression applied by the finger

Similarly as expressed on equation (2.34), the force can be calculated from the dynamic model.

$${}^{j}\mathbf{F}^{hand} = \sum_{i\in[1,2],j\in[1,2]} {}^{j}\mathbf{F}_{ti} + {}^{j}\mathbf{F}_{ni} \tag{2.72}$$

Chapter 3

Criteria of Stability

The model being completely defined, it is possible to express the conditions of stability for the design of an under-actuated system. Using existing literature, it has been chosen to follow some existing criteria for the design. In particular for the static stability condition, the existing literature was used. For what it may concern dynamics, new criteria of stability are defined. Moreover, as we have a moving gripper, some kinematics constraints must be taken into account.

3.1 Kinematic Constraint

A robot of any kind can meet singularities. A singularity is an instantaneous loss of degree of freedom of the mechanism or degree of actuation. This is a problem, because on such a a case, the configuration of the robot cannot be controlled any more. In particular for the gripper, it is possible that for some specific precise configuration, no effort could be applied with the distal phalanx or that their is no solution to achieve the desire motion.

3.1.1 Serial singularity

The first type of singularity is the serial singularity. It appends when the matrix $\mathbf{B}$, defined on equation (2.10), becomes singular.

The conditions corresponding to the case singularity occurs is expressed on equation (3.1) to (3.4).

$$q_{12}^{sing1} = 0 \tag{3.1}$$
$$q_{22}^{sing1} = 0 \tag{3.2}$$
$$q_{12}^{sing2} = \pi \tag{3.3}$$
$$q_{22}^{sing2} = \pi \tag{3.4}$$

In order to ensure that we will never reach those singularity, a security coefficient of 30° is used. If any angle is in the range presented on next equation the design is discarded.

$$q_{i2}^{singj} - 30° < q_{i2} < q_{i2}^{singj} + 30° \quad i \in [1,2], j \in [1,2] \tag{3.5}$$

3.1.2 Parallel singularity

The parallel singularity appears when the matrix $\mathbf{A}$, defined on equation (2.9), becomes singular. The link 12 and 22 are aligned. The following equation defines the condition of singularity.

$$q_{13}^{sing1} = 0 \tag{3.6}$$

$$q_{13}^{sing2} = \pi \tag{3.7}$$

Similarly, a security limitation of 30° is used. the condition used to discard some models is shown on the following equation.

$$q_{13}^{singj} - 30° < q_{13} < q_{13}^{singj} + 30° \quad j \in [1, 2] \tag{3.8}$$

3.2 Static criteria

Before to define the dynamic condition, it is important that the static condition are verified. This will moreover ease the analysis of dynamics because the area of research will be tremendously reduce by the static study. Two criteria of stability

3.2.1 Palm force positiveness and force positiveness

The condition of palm force positiveness is checked both for the case where no offset are taken into account or if their is one. The condition is checked if the following expression is checked for all configuration.

$$F_y < 0 \tag{3.9}$$

Similarly, the force positiveness is checked by using the relation 1.1.

3.2.2 Form closure

The first criteria is the form closure property. Firstly adapted to a non underactuated gripper, this property has been generalised to all type of gripper in [10]. In the master thesis [11], this definition has been explained to. The definition given is the following one:

> *"A grasp is said to be form-closed if, and only if, for any variation of the configuration of the grasp at least one of the unilateral kinematic constraints is violated."*

A short explanation is given here to define mathematically this condition. A matrix has been defined to express this condition mathematically. This matrix comes in fact from three equations.

The two first equations express the non penetration and the non backdriveability of the mechanism. Those are necessary condition for form closure with underactuated system. The last one expresses the condition of form closure for non underactuated system. This condition expresses the degrees of liberty of the object directly blocked in a geometric way. The normal of each point of contact prevent some degree of freedom.

The condition of non penetration can be expressed for a completely actuated system with the general relation given on equation (3.10). If the condition is checked, the six degree of freedom are prevented geometrically.

$$\underline{\mathbf{n}}_i \dot{\mathbf{q}} \geq 0 \quad with : \underline{\mathbf{n}}_i = \begin{bmatrix} \mathbf{I}_3 \\ \hat{\mathbf{p}}_i \end{bmatrix} \mathbf{n}_i \tag{3.10}$$

With:

- $\hat{\mathbf{p}}_i$ the cross-product of vector $\mathbf{p}_i$
- $\mathbf{p}_i$ is the vector going from the origin attached to the palm to the point of contact
- $\mathbf{n}_i$ the normal vector on the point of contact

In the case of an underactuated system, it can be expressed with relation (3.11).

$$\dot{\mathbf{q}}_c = \mathbf{M}_c \boldsymbol{\omega}_g = \begin{bmatrix} \mathbf{S}_s \mathbf{P}_n & -\mathbf{S}_s \mathbf{J}_1 \\ \mathbf{0}_{2,2} & \mathbf{K} \\ \mathbf{n}_p^T & \mathbf{0}_{1,2} \end{bmatrix} \begin{bmatrix} \dot{\mathbf{q}} \\ \dot{\boldsymbol{\theta}} \end{bmatrix} \tag{3.11}$$

With:

- $\mathbf{M}_c$ is the matrix of form closure.
- $\mathbf{q}$ is the vector of generalised coordinates of the object.
- $\boldsymbol{\theta}$ is the vector of all angle θ_i defining link position.
- $\mathbf{q}_c$ is a control angle checking all constraints.
- $\mathbf{S}_s$ is a selection matrix of touching phalanx.
- $\mathbf{P}_n = \begin{pmatrix} {}^1\mathbf{P}_n^T & {}^2\mathbf{P}_n^T \end{pmatrix}^T$ is the gathering of the projection matrix relative to normal forces of both finger.
- $\mathbf{J}_n = \begin{pmatrix} {}^1\mathbf{J}_n^T & {}^2\mathbf{J}_n^T \end{pmatrix}^T$ is the gathering of the Jacobian matrix relative to normal forces of both finger.
- $\mathbf{K}$ is the matrix of non backdrivebility constructed from the first row of the transmission matrix ${}^i\mathbf{T}$ of the two fingers.
- $\mathbf{n}_p = [\ 0 \quad 1\ ]^T$ is the matrix expressing the condition of non penetration into the palm.

Once the matrix $\mathbf{M}_c$ has been determined, it is possible to plot what is called the convex hull of the matrix. It expresses the possibility of the object to go in one or more direction. We know the main directions on which the object can go thanks to the expression (3.10). From this and expressions of other constraints in (3.11), we evaluate a matrix and can then extrapolate to all directions. The convex hull is the area on which the geometry block the object to grasp. From this, we can say that an object will be considered as form closed if the origin of the convex hull spaces (position of equilibrium) is completely included in the convex hull. To illustrate it, the convex hull for two matrices is presented in [1]. The figure 3.1 presents the results for two grasps. On figure 3.1(a), the origin is inside the convex hull. Any motion of the object are prevented on the direction x_1, x_2 and u_x. The grasp performs a form closure. In the case (b), the origin is on the edge of the convex hull, some direction are not prevented, there is not a first order form closure.

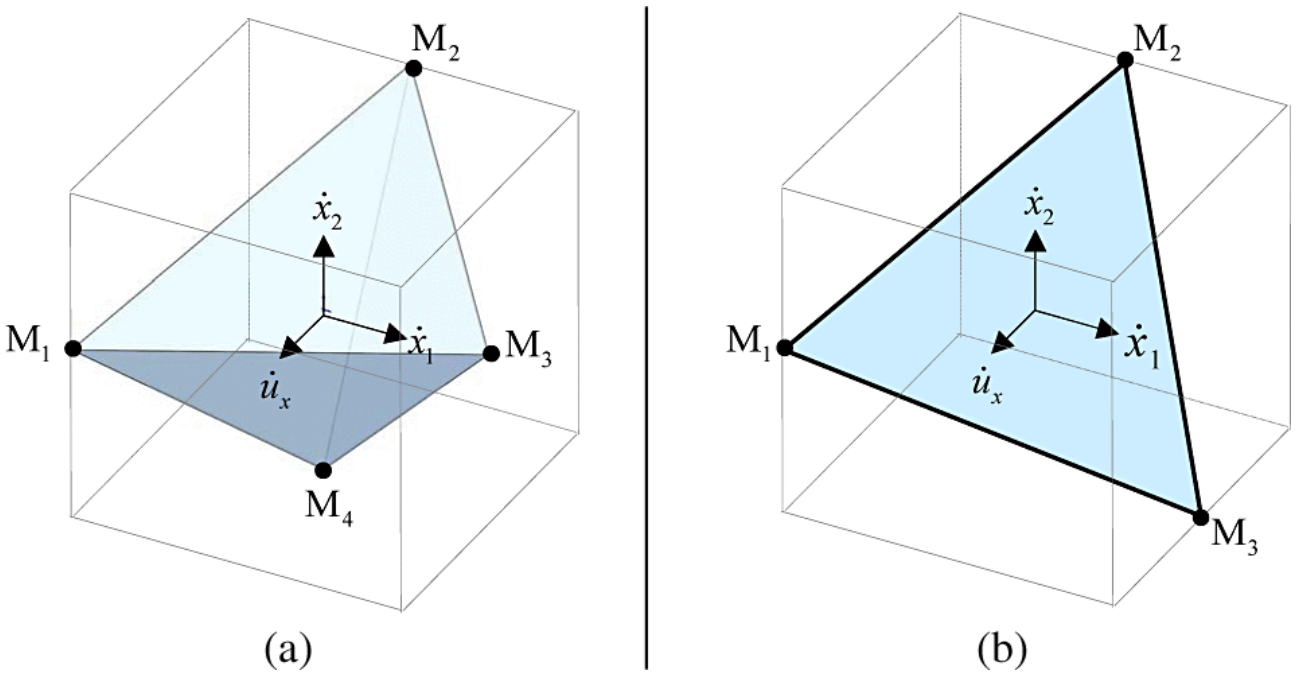

Figure 3.1: (a) convex hull of a first mechanism which is form closed (b) convex hull of a mechanism which is not form closed. Extracted from [1]

.

3.2.3 Force isotropy and maximisation of applied forces

In order to have a good design, two important conditions are necessary. First it is necessary that the forces applied on the object must be as high as possible. That is why we will evaluate the average force $\tilde{F}$ of the normal forces f_i applied on the object and try to maximize it.

Secondly, the forces must be as equal as possible. The index α defined on equation (3.12). A similar index was first defined in [14]. This index has been adapted to prevent that the index raise when the forces raise. It has been normed to do it. This index will tends to zero if the finger is isotropic. It will tend to infinity if the force positiveness is not achieved. This way the roll back phenomenon will be prevented.

$$\alpha = \frac{(\tilde{F} - f_1)^2 + (\tilde{F} - f_2)^2}{f_1 f_2} \tag{3.12}$$

With :

- $\tilde{F}$ the mean force of f_1, f_2.
- f_i the normal force of phalanx i.

The index α should be minimized.

3.3 Dynamic criteria of stability

Once the static stability has been checked, and the number of design reduced, it is possible to study the dynamic stability. To do this, a simulation is created. This simulation takes as input the torque and the design of the gripper. The direct dynamic model gives the joint coordinates acceleration. By integration, the joint coordinates and velocity are obtained. From the kinematics and geometry, the forces of contact are computed. The dynamic model takes then those forces into account.

We can say that the dynamic stability will be checked if the object did not move from impacts or from forces and if the static stability is obtained at the end of the simulation. All previous criteria are then checked during or at the end of the simulation. New criteria of instability are defined to check that the cylinder is not moving or, for impacts, not to much.

3.3.1 Impact criteria of stability

The objective in this part is to define an energetic criteria to know if the cylinder is moving to much or not. The cylinder can move in two ways. As said previously, it can rotate or translate. By knowing the energy of the cylinder after the impact, we will be able to know if the cylinder will stop quickly due to other forces or not. Two questions remain then. What is the energy transferred to the cylinder after the impact and from which energy can we say that the cylinder is moving to much.

Expression of energy after impact

The first question is answered in [20]. In this part, the general idea is reminded quickly. We will consider in this part that only one contact occurs at the moment of impact, and this impact is made by the proximal phalanx. Moreover we consider that the cylinder is orthogonal to the ground and hand plane. The cylinder is previously in a static equilibrium. Moreover the contact of the cylinder with the ground is forgotten, living the cylinder completely free. The gravity, and torques are neglected because the contact is supposed instantaneous.

The general equation of dynamics for all the system composed of the cylinder and the finger can be written under the form presented on equation (3.13).

$$\mathbf{M}_s\ddot{\mathbf{q}}_a^s + \mathbf{c}_s = \boldsymbol{\tau}_s + \mathbf{A}_b^T\boldsymbol{\lambda}_b + \mathbf{A}_u^T\boldsymbol{\lambda}_u \tag{3.13}$$

With :

- $\mathbf{q}_a^s$ is the generalised coordinates vector for the system;
- $\mathbf{M}_s$ is the inertia matrix;
- $\mathbf{c}_s$ the matrix of Coriolis and centrifugal effect.
- $\mathbf{A}_b = \frac{\partial \boldsymbol{\Phi}_b}{\partial \mathbf{q}}$ is the Jacobian matrix corresponding to bilateral constraints $\boldsymbol{\Phi}_b(\mathbf{q}) = \mathbf{0}$;
- $\mathbf{A}_u = \boldsymbol{\Gamma}_c\frac{\partial \boldsymbol{\Phi}_u}{\partial \mathbf{q}}$ is the Jacobian matrix corresponding to unilateral constraints $\boldsymbol{\Phi}_u(\mathbf{q}) \geq \mathbf{0}$ with $\boldsymbol{\Gamma}_c$ a diagonal matrix equal to 0 or 1 depending if the constraint is applying;
- $\boldsymbol{\lambda}_b$ and $\boldsymbol{\lambda}_u$ are the Lagrangian multipliers associated to bilateral or unilateral constraints;
- $\boldsymbol{\tau}_s$ the vector of external forces applied on the system;

This theory is applied to the case of one finger touching the cylinder with its proximal phalanx. On figure 3.2, the object and the first Phalanx are represented. We want to evaluate the energy of the cylinder after the impact. As it is an impact the time period of the finger touching the object is very short. The movement of the cylinder is then in the plane normal to x_{21}. Only three variables are then sufficient to evaluate the motion of the cylinder. The chosen generalised coordinates associated to the cylinder are then $\mathbf{q}_a^{cyl} = \begin{pmatrix} x_c & y_c & \theta \end{pmatrix}^T$. x_c and y_c are the coordinates of the center of gravity of the cylinder, θ its angle around axis x_{21}.

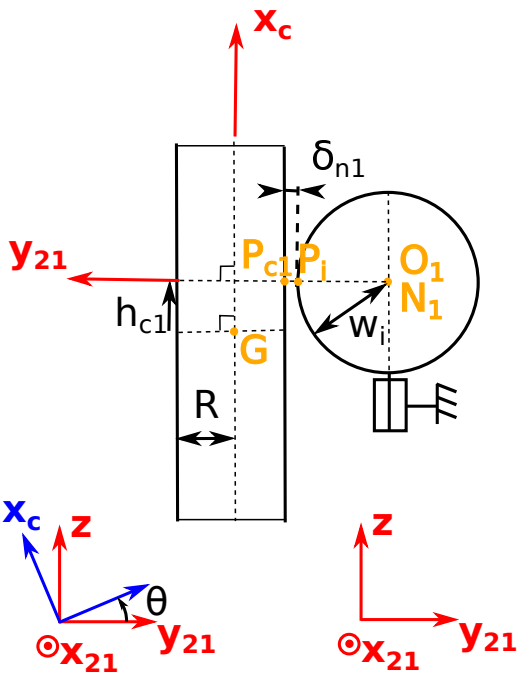

Figure 3.2: Geometry and notations of cylinder contact

Finally we can evaluate the inertia matrix associated to the system composed of the cylinder and of the finger presented on equation (3.14) and associated to the generalised coordinates $\mathbf{q}_a^s = \begin{pmatrix} \mathbf{q}_a^T & \mathbf{q}_a^{cyl^T} \end{pmatrix}^T$.

$$\mathbf{M}_s = \begin{pmatrix} M_{11} & M_{12} & 0 & 0 & 0 \\ M_{21} & M_{22} & 0 & 0 & 0 \\ 0 & 0 & m_c & 0 & 0 \\ 0 & 0 & 0 & m_c & 0 \\ 0 & 0 & 0 & 0 & J_c \end{pmatrix} \tag{3.14}$$

M_{ij} are the coefficient of the inertia matrix of the finger $\mathbf{M}$ computed on equation (2.47). m_c is the mass of the cylinder, J_c is the inertia of the cylinder on its center of gravity along an axis orthogonal to the direction of the cylinder.

The constraint equation at the moment of impact can be expressed and derived to obtain the equation (3.15).

$$k_1 \dot{q}_{21} - \dot{y}_c + k_c \dot{\theta} = 0 \tag{3.15}$$

The unilateral constraint can then be expressed under the relation given on equation (3.16).

$$\mathbf{A}_s = \begin{pmatrix} 0 \\ k_1 \\ 0 \\ -1 \\ k_c \end{pmatrix} \tag{3.16}$$

By applying the theory given in [20], the matrix used for the definition of velocity after

impact in equation (1.22) is obtained on equation (3.17) from the matrix $\mathbf{A}_s$ and $\mathbf{M}_s$.

$$S = m_{tot} \begin{pmatrix} 0 & -\frac{M_{21}}{M_{11}}\frac{1}{m_{finger}} & 0 & \frac{1}{k_1}\frac{M_{21}}{M_{11}}\frac{1}{m_{finger}} & -\frac{k_c}{k_1}\frac{M_{21}}{M_{11}}\frac{1}{m_{finger}} \\ 0 & \frac{1}{m_{finger}} & 0 & -\frac{1}{k_1}\frac{1}{m_{finger}} & \frac{k_c}{k_1}\frac{1}{m_{finger}} \\ 0 & -k_1\frac{1}{m_{trans}} & 0 & \frac{1}{m_{trans}} & -k_c\frac{1}{m_{trans}} \\ 0 & 0 & 0 & 0 & 0 \\ 0 & \frac{k_1}{k_c}\frac{1}{m_{rot}} & 0 & -\frac{1}{k_c}\frac{1}{m_{rot}} & \frac{1}{m_{rot}} \end{pmatrix} \tag{3.17}$$

In this process, some new equivalent masses are defined. First the matrix m_{rot} which will give the energy given in rotation to the cylinder, m_{trans} which will give the energy in translation to the cylinder, and m_{finger} corresponding to the finger equivalent mass.

$$\begin{aligned} m_{rot} &= J_c/k_c^2 \\ m_{trans} &= m_c \\ m_{finger} &= \frac{M_{11}M_{22} - M_{12}^2}{M_{11}k_1^2} \end{aligned}$$

We can then get the equivalent mass associated to the cylinder on equation (3.18).

$$m_{cyl} = \frac{m_{trans}m_{rot}}{m_{trans} + m_{rot}} \tag{3.18}$$

We can note here that if we get the velocity in projection along the contact normal of both the object, the shock energy and the velocity after impact of those two points will be equivalent if two spheres were launched against each other of mass m_{cyl} and m_{finger} respectively.

The total equivalent mass is then defined on equation (3.19)

$$m_{tot} = \frac{m_{finger}m_{cyl}}{m_{finger} + m_{cyl}} \tag{3.19}$$

We can then obtain the energy given to the cylinder, in translation or in rotation thanks to the matrix $\mathbf{S}_c$ and the relation (1.22). The obtained energy of the cylinder after impact is presented on equation (3.20).

$$E_{cyl}^+ = \frac{m_{tot}^2}{m_{cyl}} V_{impact}^2 (1+e)^2 \tag{3.20}$$

The energy in translation after the impact of the cylinder defined as $E_{trans} = \frac{1}{2}m_c(\dot{x}_c^2 + \dot{y}_c^2)$ is given on equation (3.21).

$$E_{trans}^+ = \frac{m_{tot}^2}{m_{trans}} V_{impact}^2 (1+e)^2 \tag{3.21}$$

Similarly we can obtain the energy in translation defined as $E_{rot} = \frac{1}{2}J_c(\dot{\theta})$ after the impact.

$$E_{rot}^+ = \frac{m_{tot}^2}{m_{rot}} V_{impact}^2 (1+e)^2 \tag{3.22}$$

For the finger, we can obtain the general coordinates velocity after the impact on equation (3.24).

$$\dot{q}_{21}^+ = \dot{q}_{21}^- - (1+e)\frac{m_{tot}}{m_{finger}}\dot{q}_{21}^- \tag{3.23}$$

$$= \frac{m_f - em_c}{m_f + m_c}\dot{q}_{21}^- \tag{3.24}$$

Definition of the criteria

The idea here is simple. Once we know the energy of the cylinder, we can tell if it goes only in translation or rotation, the maximum distance it will reach or the maximum angle it will reach. For the rotation the gravity only goes against the movement. For the translation, the friction prevent the object to go to far.

The first case correspond to the case where all energy is given in translation. The energy taken out by friction is then given on equation (3.26).

$$W_{fric} = -\int_0^{t_f} \mu_d m_c g dt \tag{3.25}$$

$$= \mu_d m_c g \Delta x_G \tag{3.26}$$

Given a maximum displacement, we can evaluate the maximum energy the cylinder should have. The resulting criteria, is given on equation (3.27).

$$E_{cyl} < \Delta x_G^{max}(\mu_d m_c g - f_n) \tag{3.27}$$

The second case correspond to the case where all the energy is transferred in translation. We can evaluate the potential energy of the cylinder for an angle θ_c. The resulting energy is given on equation (3.28).

$$\Delta E_p = \frac{m_c g L_c}{2}\left(\cos(\theta_c) - 1\right) + R_c m_c g \sin(\theta_c) \tag{3.28}$$

In that case, we can evaluate the maximum energy we can give to the cylinder before the maximum defined angle θ_c is reached. The maximum energy is given on equation (3.29).

$$E_{cyl} < \frac{m_c g L_c}{2}\left(\cos(\theta_c^{max}) - 1\right) + R_c m_c g \sin(\theta_c^{max}) \tag{3.29}$$

3.3.2 Force criteria of cylinder stability

No we know that the cylinder won't move to much after an impact, the question is will the cylinder move when the contact remains a long time. This condition must be checked in any configuration of the hand.

This criteria will be useful in particular when no bounce will appear after the first contact happened. The force applied by the phalanx could push the object, the finger keeping their movement of closure. It is then possible that the object would finish by being out of reach for the gripper. This must be avoided at any cost.

Two different phenomena could appear to make the cylinder move. The first would be that the object would slip on the floor and/or on the palm. The case is that the cylinder will begin to topple.

Condition to prevent slipping

The condition for the cylinder no to slip can be expressed thanks to the theory of Coulomb. To make it simple, all the forces must remain in the friction cone. If the static equilibrium equation leads to force not included in the friction cone, we will be able to conclude that the static stability condition of the cylinder is not checked. We can note here that the forces applied on the cylinder could but come from the dynamic model of the finger.

To begin with, we define the condition of stability for the cylinder on equation (3.30) and (3.31).

$$\left\|\mathbf{F}_t^{Palm}\right\| < \mu_p F_n^{Palm} \tag{3.30}$$

$$\left\|\mathbf{F}_t^{Ground}\right\| < \mu_g F_n^{Ground} \tag{3.31}$$

With :

- F_n^{Palm} and $\mathbf{F}_t^{Palm}$ the normal force norm and tangential force exerted by the object on the palm.
- F_n^{Ground} and $\mathbf{F}_t^{Ground}$ the normal force norm and tangential force exerted by the object on the ground.
- μ_p the static friction coefficient between the palm and the object.
- μ_g the static friction coefficient between the palm and the object.

The difficulty of the problem come from the fact that the cylinder is generally statically indeterminate because of many efforts applied on the object. We suppose then than if no forces are applied, all components are null except the normal force of the ground which compensate for gravity. It means that there is no pre-charge in the system.

We will consider that the gravity is compensated by the ground only:

$$F_n^{Palm} = \mu_g m_c g \tag{3.32}$$

Moreover for the palm, we know that no penetration is possible. We then have inequality (3.33). Moreover we guess that the palm does not support here any effort along the $\mathbf{z}$ axis.

$$F_n^{Palm} \geq 0 \tag{3.33}$$

The total force applied on the object by the fingers can be found using the dynamic model of the fingers an considering the cylinder as fixed. It is obtained by taking the sum of all forces applied on the cylinder by the different phalanges. The sum of forces is considered to be in the plane of the finger which is supposed to be parallel to the ground and orthogonal to the axe of the cylinder. We note the sum of forces as $\mathbf{F}^{hand} = \begin{pmatrix} F_x & F_y & 0 \end{pmatrix}$.

The static equilibrium equation is then presented on equation (3.34).

$$\begin{cases} F_x + F_t^{Palm} + \mathbf{F}_t^{Ground} \cdot \mathbf{x} = 0 \\ F_y + F_n^{Palm} + \mathbf{F}_t^{Ground} \cdot \mathbf{y} = 0 \end{cases}$$

In the case where the force F_y is positive, the condition is simple. The force F_{Palm}^n and F_{Palm}^t are null as there is no pre-charge, the limit is then given on equation (3.34) to check equation (3.31).

$$F_y^2 + F_x^2 < (\mu_g m_c g)^2 \tag{3.34}$$

In the case where the force F_y is negative, both the ground and the palm compensate for the forces. We then have the condition (3.35)

$$|F_x| < -\mu_p F_y + \mu_g m_c g \tag{3.35}$$

Condition to prevent toppling

To prevent the rotation, the theorem of moment is applied at the basis of the cylinder on the furthest point in the direction of $\mathbf{F}^{hand}$. It would be the point of rotation if the cylinder begin to rotate.

It can be shown that the condition for F_y positive or negative has then similar expression and written as shown on equation (3.36).

$$\begin{cases} Cond : F_y^2 + F_x^2 < \left(\frac{R_c m_c g}{h}\right)^2 & if \quad F_y > 0 \\ Cond : |F_x| < -\mu_p F_y + \frac{R_c m_c g}{h} & else \end{cases} \tag{3.36}$$

With :

- R_c the radius of the cylinder.
- m_c the mass of the cylinder
- h_f the height of the finger from the ground.

We can note here that this criteria is not dependant of the height of the object.

Conclusion on force stability

Finally we can define a radius of stability for the forces defined on equation (3.37).

$$R_{area} = min(\mu_g m_c g, \frac{R_c m_c g}{h}) \tag{3.37}$$

We then have the following condition :

$$\begin{cases} Cond : F_y^2 + F_x^2 < R_{area}^2 & if \quad F_y > 0 \\ Cond : |F_x| < -\mu_p F_y + R_{area} & else \end{cases} \tag{3.38}$$

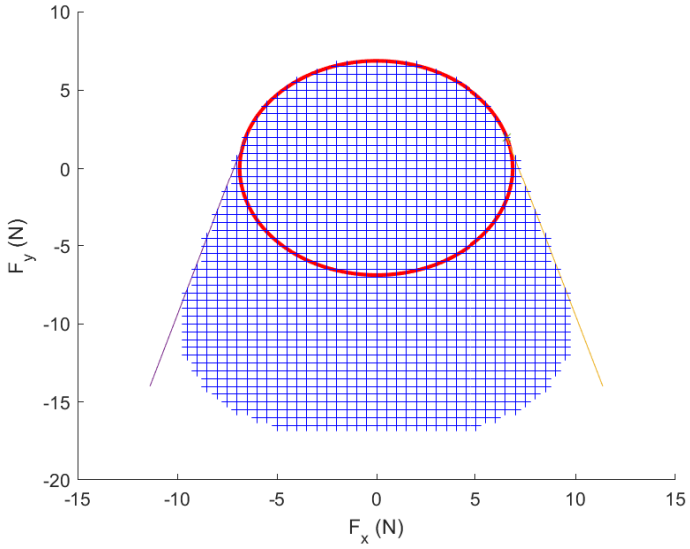

Figure 3.3: Contact Forces on the finger

The area of stability can then be observed on figure 3.3. During the grasping process, the palm force positiveness must not be obligatory checked. Only when the stability of the complete hand is obtained, this criteria will be important.

3.3.3 Definition of the time to stability

The time to stability is the time going from the beginning of the simulation to the moment we can say we reached the static stability. If no singularities were found, if the previously defined criteria didn't lead do an instability, it is possible to wait until the stability is reached. To be able to say that the static equilibrium is reached, two criteria are used, depending on the case where bounce occurs or not. The final time of the simulation is kept and defined as the time to stability.

Bounce limit criteria

The bounce analysis gives the ability to stop the simulation once before we obtain the perfect static equilibrium. Indeed, if the coefficient of restitution is high, the amplitude of bounces could be very low with still important acceleration due to impact forces. It has then been chosen to stop the simulation if the amplitude of all generalised coordinates bounce are inferior to 5% of the maximum one. Moreover we check that all bounces amplitude were reduced from the last ones. By taking the final time of the simulation, we obtain a time to stability.

Acceleration limit criteria

Similarly, if no bounce occurs, we have to check that the accelerations are low enough for all generalised coordinates. If the accelerations are bellow a threshold, the simulation is stopped and the time to stability are obtained.

Chapter 4

Simulation analysis

4.1 General methodology

The objective of the project is to find a methodology of design for the gripper. A set of variable give the possibility to design the gripper. Some of those variable will be chosen before the complete design is chosen. The first step is to remove some variable in order to simplify the problem. Then step by step the analysis will give the possibility to see which parameter has an influence on which criteria. The objective would be at the end of this report to propose a design methodology according to the results presented in this section.

4.1.1 Reduction of the number of variable

The first step consist to discard some parameter from the analysis.

Width of fingers

The first parameter chosen as a constant is the width of the finger. Indeed it has been shown in [6] that anyway, they will be a better stability in dynamic if the width is reduced to its minimal value. The width will then be chosen thanks to the technological limits. The chosen value is $w = 5mm$.

Choice of initial configuration

The choice of initial configuration will influence the dynamic results. In particular as a constant torque is imposed as an input, the impact energy will depend on both initial joint coordinates. To be able to compare the different design initial configuration is chosen.

Initial joint position The first parameter chosen is the angle q_{22_0} such as the finger is completely open at initial time step. The relation (4.1) appears then for the finger on the right.

$$q_{22_0} + \psi = 0 \tag{4.1}$$

Then the initial angle q_{21_0} is chosen. This angle must be chosen such as the finger do not touch the object at initial position. It has then been chosen that the initial position will correspond to the case the proximal phalanx will be tangent to a cylinder of radius $R_c^{max} = 10cm$. The equation 4.2 gives the initial angle with k_{1_0} defined on equation 4.3 corresponding to the length of contact of the first phalanx in the case the object were of radius R_c^{max}.

$$q_{21_0} = \pi - \tan^{-1}\left(\frac{2R_c^{max}}{b}\right) - \tan^{-1}\left(\frac{R_c^{max}+w}{k_{1_0}}\right) \tag{4.2}$$

$$k_{1_0} = \sqrt{\left(\frac{b}{2}\right)^2 + (R_c^{max})^2 - (R_c^{max}+w)^2} \tag{4.3}$$

The initial angle q_{11_0} is finally chosen such as $q_{21_0} = q_{11_0} + \frac{\pi}{2}$.

Finally the whole configuration of the finger has been chosen. Those conditions are even redundant leading to the relation (4.4).

$$l_{12} = \left\| l_{21}\mathbf{x}_{21_0} + l_{22}\mathbf{x}_{22_0} - \overrightarrow{\mathbf{O}_{21}\mathbf{O}_{11}} - l_{11}\mathbf{x}_{11_0} \right\| \tag{4.4}$$

Spring dimensioning

The choice of the spring is very important. The increase of the spring stiffness will create an instability on the grasp. Indeed, if we take the critical case with a very high stiffness, the finger won't even close. So if it is a bit to high, the design will result in a law force exerted on the distal phalanx. And will result to no palm force positiveness. If by opposition, the spring stiffness is too low, undesired motion could appear at high acceleration or due too gravity. In particular, the distal phalanx could fold before any contact.

To overcome any problem a methodology has been created and used in the design of the gripper. It is first possible to define an upper and a lower bound for the spring stiffness. As the increase of the stiffness will result in a less good design, it has been chosen to select the lower bound for the design.

Lower bound for the spring stiffness To express the lower limit, the condition we express is the following one. We do not want the distal phalanx to fold before it touches the object. This condition give the possibility to link the torque to the wanted spring stiffness. To do it, we start from the dynamic model of the system. The equations (4.5) and (4.6) gives the system dynamics.

$$\ddot{\mathbf{q}}_a = \mathbf{M}^{-1}(\boldsymbol{\tau} - \mathbf{c}) \tag{4.5}$$

$$\ddot{\mathbf{q}}_d = \mathbf{J}_d\ddot{\mathbf{q}}_a + \mathbf{J}_{td}^{-1}\mathbf{d}_c \tag{4.6}$$

A first assumption is done here. The Coriolis and centrifugal effect are neglected to simplify the problem. Then, the velocity must not be to high. As the velocity is initially null, this condition is valid a the beginning. This assumption will result in the fact that the distal phalanx could begin to close softly before the distal phalanx touch the object. This assumption is simply checked after, using the dynamic model, by evaluating the distal angle variation and checking that it is under 5 degree when the first contact occurs.

This assumption leads to the equation (4.7).

$$\ddot{\mathbf{q}}_d = \mathbf{J}_d\mathbf{M}^{-1}\boldsymbol{\tau} \tag{4.7}$$

The vector of external forces exerted on the finger is due to two forces: the torque applied and the spring. There is no internal contact because, the extremal case is taken, the distal phalanx is at the limit to fold. Moreover, their is still no contact with the object.

The resulting torque can be expressed by the equation (4.9)

$$\boldsymbol{\tau} = \begin{pmatrix} \tau_1 \\ 0 \end{pmatrix} + \mathbf{J}_d^T \begin{pmatrix} 0 \\ \tau_{s22} \end{pmatrix} \tag{4.8}$$

$$\boldsymbol{\tau} = \begin{pmatrix} \tau_1 + J_d^{21}\tau_{s22} \\ J_d^{22}\tau_{s22} \end{pmatrix} \tag{4.9}$$

The acceleration of the passive joint is then obtained on equation (4.10).

$$\ddot{\mathbf{q}}_d = \mathbf{J}_d\mathbf{M}^{-1} \begin{pmatrix} \tau_1 + J_d^{21}\tau_{s22} \\ J_d^{22}\tau_{s22} \end{pmatrix} \tag{4.10}$$

To obtain the condition that the distal phalanx does not close before the proximal phalanx touch the object, the variable $\dot{q}_2 2$ should be positive (respectively negative) or equal to zero for the finger on the right (respectively on the left). The limit case is obtain when it is equal to zero.

In the case where no assumption are taken for the geometry, the condition where this condition will be validated for a particular initial angle. That is why the choice has been made to take as an assumptions that the point O_{11} and O_{12} are coincident.

In that case, the matrix $\mathbf{J}_d$ becomes singular. If we want to have a null velocity of the passive joint at the limit of contact, we have to find the kernel of $\mathbf{J}_d\mathbf{M}^{-1}$. This way we find:

$$J_d^{22}\tau_{s22} = \frac{M_{22} + M_{12}}{M_{11} + M_{12}}(\tau_1 + J_d^{21}\tau_{s22}) \tag{4.11}$$

With :

- $\mathbf{M} = \begin{pmatrix} M_{11} & M_{21} \\ M_{21} & M_{22} \end{pmatrix}$
- $\mathbf{J}_d = \begin{pmatrix} J_d^{11} & -J_d^{11} \\ J_d^{21} & -J_d^{21} \end{pmatrix}$

Finally the condition to have a null acceleration for the passive angle, and then being at the limit of contact, can be expressed by a choice of a particular spring torque as shown on equation (4.12).

$$(\frac{M_{11} + M_{12}}{M_{22} + M_{12}}J_d^{22} - J_d^{21})\tau_{s22}^{min} = \tau_1 \tag{4.12}$$

4.1.2 Variable chosen for the complete analysis

In order to chose the design of the gripper, some of the parameter must be chosen. In particular, the physical properties of the finger and object must be chosen. The list of all the parameter is presented here.

- $\mu_s = 0.6$ the static coefficient of friction between the object and the hand;
- $\mu_d = 0.4$ the dynamic coefficient of friction between the object and the hand;
- $v_s = 510^{-3}m \cdot s^{-1}$ and $v_d = 1010^{-3}m \cdot s^{-1}$, the static and dynamic transition; velocities for the expression of the continuous friction;
- $\mu_g = 0.4$ the dynamic coefficient of friction between the object and the ground;

- $\mu_p = 0.5$ the static coefficient of friction between the object and the palm;
- $e = 0.3$ the restitution coefficient between the object and the hand;
- $K = 5.310^8 N \cdot m^{-3/2}$ the contact stiffness between the object and the hand;
- $\rho_c = 1000kg \cdot m^{-3}$ the density of the cylinder;
- $\rho_f = 1380kg \cdot m^{-3}$ the density of the finger;
- $w = 5mm$ the finger phalanges and links radius;
- $R_c = 40mm$ for the static and dynamic analysis, $30mm$ and $50mm$ for the singularity avoidance;
- $L_c = 200mm$ the length of the cylinder;
- $h_c = 50mm$ the height at which the cylinder is grasped.

For what it may concern the variable, the chosen variable, if they are not the studied variable are the following one :

- $\tau = 0.5Nm$ the torque applied on action link;
- $b = 56mm$ the palm length;
- $l_{21} = 49.4mm$ the length of link 21;
- $l_{hand} = 230mm$ the length of the hand $l_{hand} = b + 2t_{22} + 2l_{21}$;
- $r = 0.46$ the ratio l_{22}/l_{11} the transmission ratio;
- $p = 0.4$ the ratio l_{11}/l_{21};
- $\psi = -25.6p + 140°$ the distal angle.

4.1.3 Singularity removal

In order to avoid any bad configuration leading to a loss of forces, any singularity must be avoided. The singularities depending on the angle, a security coefficient of 30 ° has been chosen. Any design leading to a near to singularity configuration will be discarded.

The singularities are but dependant of the configuration. Two extreme cases are chosen to know if a singularity is appearing.

The first case is the case when the finger is completely open. The second case correspond to the case when the finger is closed on an object of small radius, meaning a radius of $R_c = 60mm$ corresponding to a can. It is moreover checked that the finger has the same configuration being open and closed, meaning that no singularities are crossed during the closure. It is finally verified that the mechanism can be mounted with the given parameters.

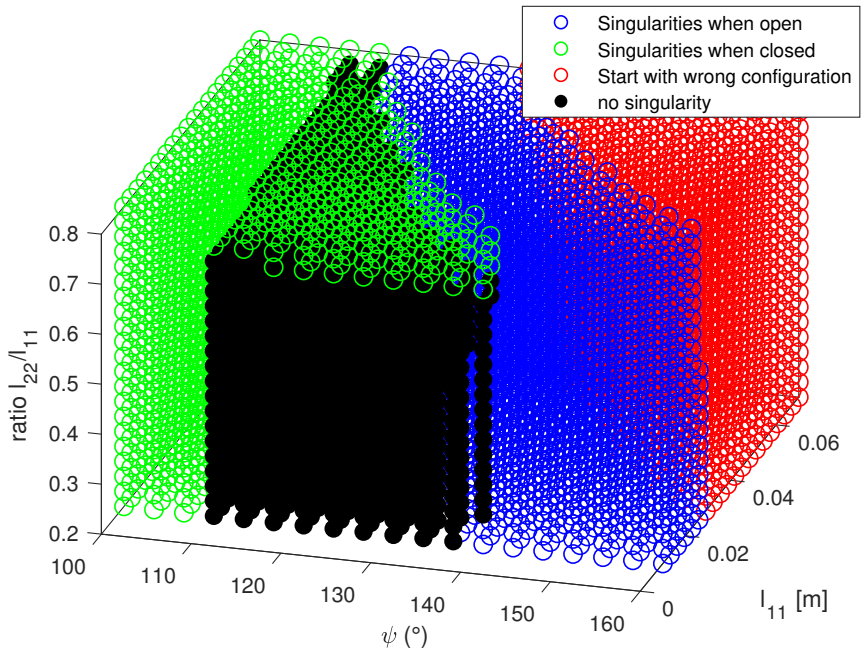

Figure 4.1: Singularities area for the variation of the parameters l_{11} l_{22} and ψ

Mutual influence of l_{11}, l_{22} and ψ To begin with, it has been chosen to study the influence of three parameters which are very linked to singularities. The length of bar l_{11}, the length or bar l_{22} and the angle ψ. On figure 4.1 the three parameters influence on singularities is studied.

Several conclusion can be done out of those results. First four situations have been detected. In blue, the initial configuration is singular. In green, the closed configuration is singular. In red, the problem comes from the initial configuration. The initial position is not singular, but has a different configuration than the one appearing when the finger is closed. The last case in black is the area where the system won't cross any singularity. First the ratio l_{22}/l_{11} has a small impact on singularities. Only a low impact is noticed for high value of l_{11}. Moreover a maximum value of 0.8 appears. In this case it is due to a serial singularity between legs 11 and 12. The main influence is but seen for the parameters l_{11} and ψ. For what it may concern the angle, it seems that a lower threshold appears around 110 °. Then we can already sea appearing a correlation between ψ and l_{11}. The high value of both parameters leads to the wrong configuration. The area where we are in the singularity appears for medium value of both. Then low value of l_{11} will lead to a larger possible area for ψ.

Mutual influence of l_{11}, l_{22} and l_{21} If the value of ψ is carefully chosen to prevent the maximum of singularity, it is possible to study the new influence of parameter l_{21} on singularities.

The value of ψ is chosen in part 4.2.2 in order to get as less singularities as possible and being function of l_{21}, of the ratio l_{11}/l_{21}.

Moreover the value of l_{11} and l_{22} are calculated from the definition of two ratios. First the transmission ratio is defined as shown on equation (4.13).

$$r = \frac{l_{22}}{l_{11}} \tag{4.13}$$

Then the length of the proximal phalanx is chosen as the reference length for the design of the links of the finger. The ratio of l_{11} over l_{21} is then defined on equation (4.14).

$$p = \frac{l_{11}}{l_{21}} \tag{4.14}$$

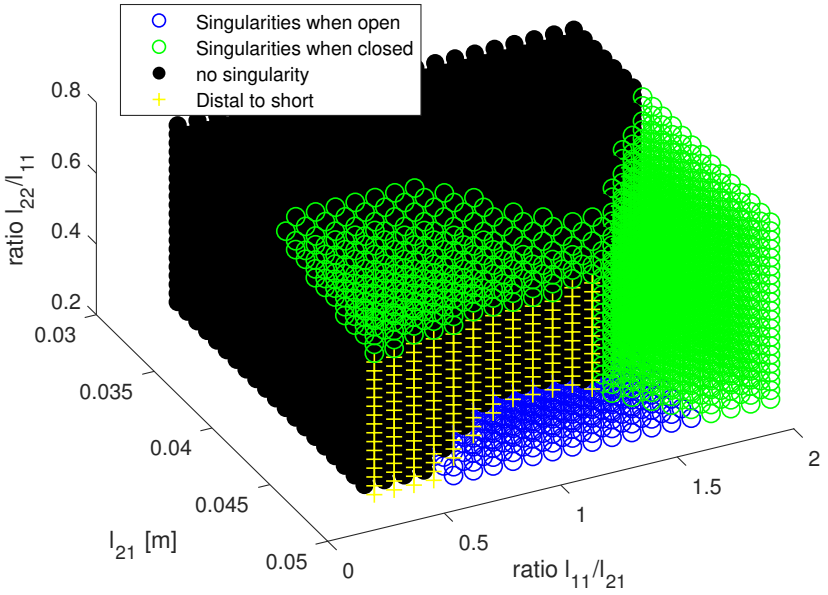

Figure 4.2: Singularities area for the variation of the parameters l_{11} l_{22} and l_{21}

The results are presented on figure 4.2 and on figure 4.3 to have a simpler vision on the results.

First a first analysis is possible from figure 4.2. We observe that higher value of l_{21} leads to the increase of singularities when the finger is closed. This seams logic as the finger distal phalanx will have to fold more if the proximal phalanx is longer. It could be argued here that maybe the choice of ψ is not optimal but it was chosen close to the critical area with $l_{21} = 0.048m$. Moreover high value of the ratio p leads to singularities if l_{21} is high. This case correspond to the appearance of the parallel singularity of the five bar linkage. Similarly high value of r leads to singularities which this time are serial singularities between body 11 and 12. The same behaviour is visible on figure 4.3, the stable area being smaller and smaller when l_{21} raise.

The analysis of figure 4.3 gives an other interesting result. The blue area is not affected by the change of l_{21}. This is due to the fact that this singularity appears before the finger is closed, and is not dependant of the object. For a ratio p around one and low value of r under 0.5 the parallel singularity appears.

It appears moreover that a maximum value of l_{21} is present. This is due too the fact that the total length of the hand were fixed. When the value l_{21} raises, the distal length of the finger reduces until the finger is not long enough to close on the object. The increase of the size of the hand will give the ability to avoid this phenomenon and possibly l_{21} could be higher than $5cm$.

Mutual influence of b, l_{hand} and l_{21} The parameter l_{11} is then chosen with a ratio equal to $p = 0.4$ and l_{22} is chosen with a ratio equal to $r = 0.47$. The angle psi is still chosen by the relation given on part 4.2.2.

The analysis can be done first without taking into account the variation of the total length of the hand l_{hand}. The case were $l_{hand} = 0.4m$ is analysed on figure 4.4.

First a minimum value of b exists, and is equal to $5cm$. The problem here is that the object must fit in the hand to touch the palm. As the finger links have a thickness, the palm length has a minimal value.

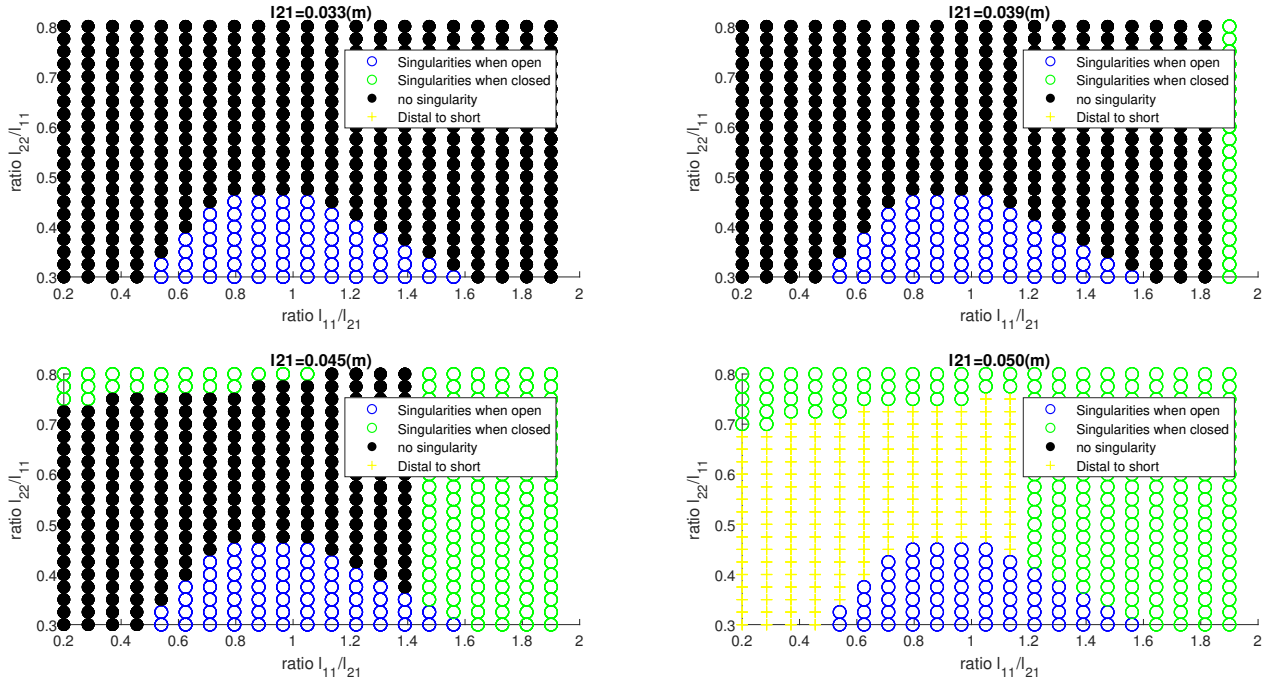

Figure 4.3: Singularities area visualised as slices for the variation of the parameters l_{11} l_{22} and l_{21}

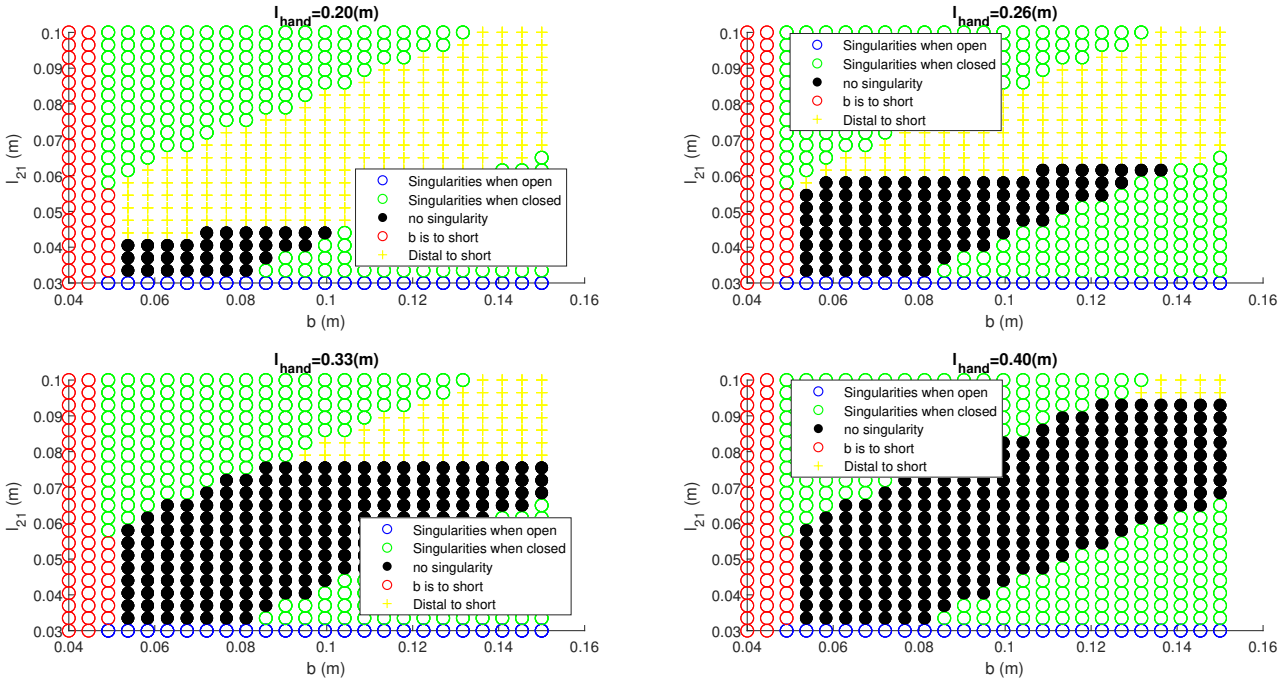

Figure 4.4: Singularities area visualised as slices for the variation of the parameters l_{hand} b and l_{21}

Then we see that l_{21} has a minimal value. This is due to the bad choice of ψ for low value of l_{21}. The parallel singularity appears. An augmentation of ψ could certainly avoid the problem.

What is more interesting is the appearing relation between b and l_{21}. It appears that a range of $4cm$ is possible for one value of b. Then when b is raising, l_{21} must raise too.

The last condition concerns now the distal length. The only condition here is that the hand must be long enough to encompass the object. For the same value of l_{hand} the value of b has nearly no influence, l_{21} must be short enough. As the length of the hand raise, the possibility for the couple b, l_{21} are extended.

Conclusion The singularities analysis leads already to some relations between some parameters. First we guess a relation between ψ and l_{11}. Two ratios have been defined, r and p. Both the ratios must not be to high with a maximum value around 0.8 for r and 1.5 for p. The lengths b and l_{21} seems to be very linked to the object and together which seems logic. l_{21} has moreover been bounded. All parameters can but still vary significantly. The static analysis will no help to reduce the range of possibilities.

4.2 Static analysis

The analysis of the design can now focus on the static conditions and forces. The same parameters will be studied in this process. The general behaviour of the hand is evaluated through three criteria. The force closure leads to a robustness of the hand, the forces applied by the distal and proximal phalanges are being equalised and the forces applied on the object are maximised.

4.2.1 Analysis of the form closure

In this part, we analyse the effect of the different design parameters on the form closure and robustness of the finger. The palm force positiveness is moreover checked but is seen here as a constraint. The robustness of the hand is moreover analysed. An offset to the object is given for this. The object can be centred, corresponding to an offset of $0mm$ or being moved on the side along the direction $\mathbf{x}$ with an offset. Two values of this offset are used, $2mm$ and $4mm$. The higher this offset is, the more restrictive for the design it will be to perform the form closure.

Analysis of parameter l_{11}, l_{22} and psi On figure 4.5, the influence of the three parameters is studied. It must be said here that the area of form closure with higher offset are included in the one of lower offset.

The first conclusion is that the parameter ψ does not influence the force closure. Only very low value of ψ could lead to a case where no palm force positiveness. We but will see in part 4.2.2 that this is not the ideal case anyway.

We then see that the parameter l_{11} leads to the same results and has no influence on the force closure.

For what it may concern the ratio r, we clearly see an impact. Only a range of r leads to a force closure. The higher the offset is, the bigger the area of form closure is. We can say that if the offset is increased further, no design can lead to the stability. Moreover, the ideal ratio r is function of ψ. The ratio decreases when ψ is increased. Then we can say that an only ratio is optimal for other given parameter defined. Among the force closure area, the ratio must be quite low, around $0.5mm$.

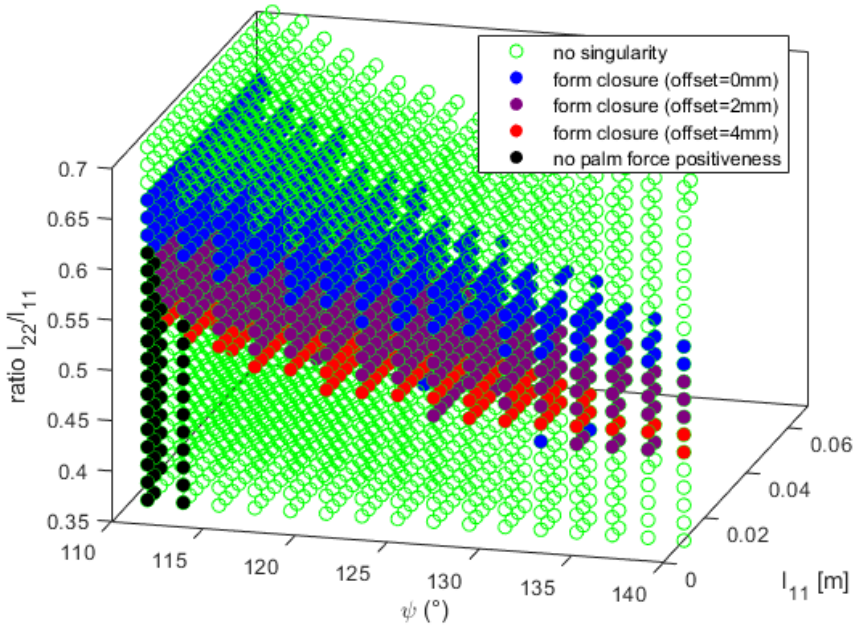

Figure 4.5: Force closure area for the variation of the parameters l_{11}, l_{22} and psi

Analysis of parameter l_{21}, l_{22} and l_{11} When the variable l_{21} is added as variable, ψ being a function of other variable, the figure 4.6 is obtained. We then see why the value of $0.05m$ was used for l_{21} when ψ was being a variable. Indeed, only high value of l_{21} leads to the case where an offset of $4mm$ leads to form closure. The ratio r is then fixed. Only the ratio p can then vary.

Analysis of parameter b, l_{21} and l_{hand} The question is then, is it possible to increase again the area where an offset of $4mm$ is possible. This figure must be looked in correlation with figure 4.4. The length of the hand l_{hand} has no influence on the area presented on figure 4.7 can but prevent certain area to be reached. For example if the value of l_{hand} is chosen as being $20mm$, the maximum value of l_{21} is then 0.045 and the red area is then not reachable.

It appears then that l_{21} must be as high as possible to increase the force closure robustness. For very low value of b, the force closure with big offset can't be achieved because the hand can't exert effort on the palm. When it is a bit increase, the purple and red areas appears, the size of the hand increases. the optimal case seems to be when b equals 0.62 the value of l_{21} being 0.065 for what it concern the robustness.

4.2.2 Analysis of the repartition of forces

In this section a torque of $0.5Nm$ was applied on the joint 11. In this section the analysis of a criteria of high forces and the index of isotropy α is carried out.

Study of the influence of parameter ψ, l_{11} and l_{22} On figure 4.8, the three parameters ψ, l_{11} and r were variable. It was but noticed that the parameter r had no influence. That is why it is not represented on this figure. This result is not obvious at first sight. This is due to the choice of the spring. As the spring is specifically chosen to be minimised for each design, the influence of the ratio r becomes null on forces. This behaviour is interesting because it will be possible to chose it to maximise the force closure.

The first thing to notice on both 4.8a and 4.8b is that a relation exist between ψ and l_{11}.

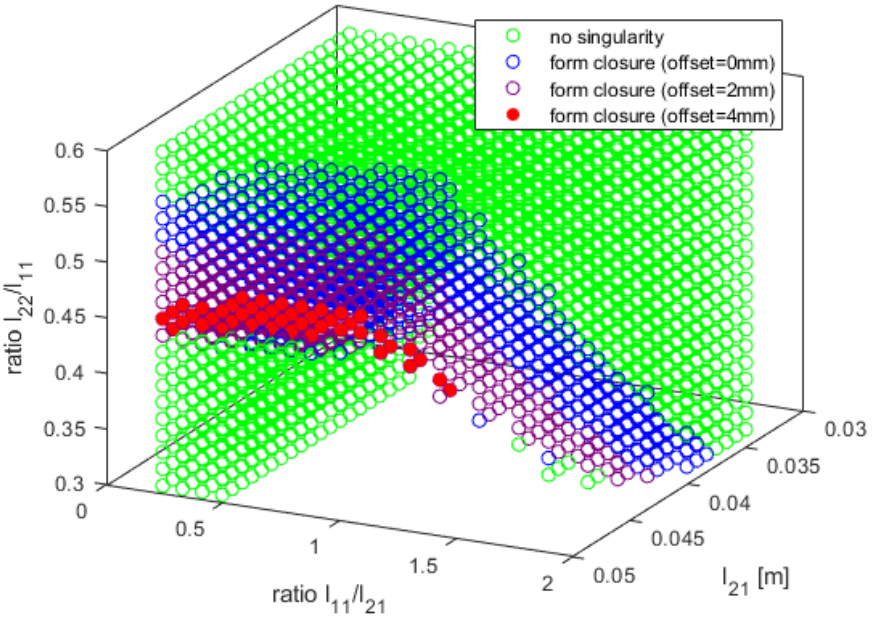

Figure 4.6: Force closure area for the variation of the parameters l_{11} l_{22} and l_{21}

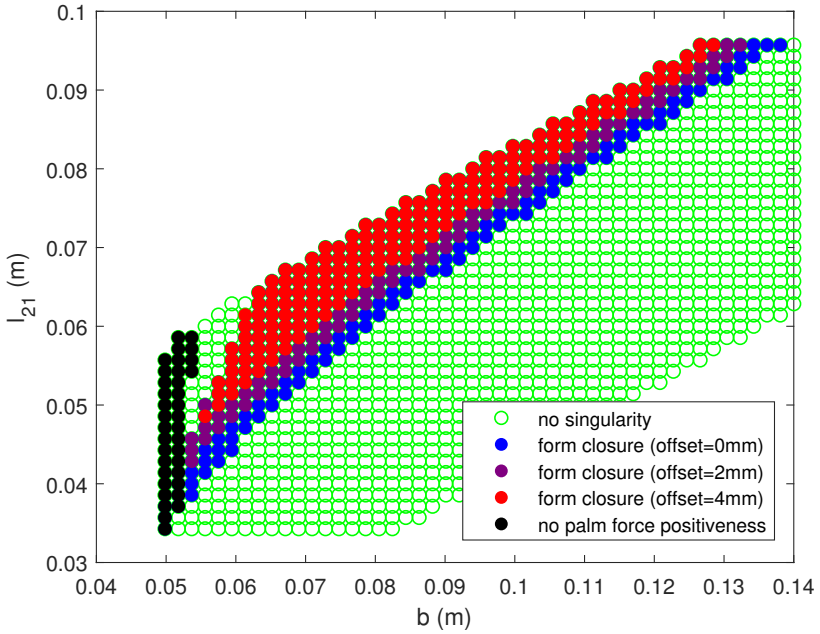

Figure 4.7: Force closure area for the variation of the parameters b, l_{21} and l_{hand}

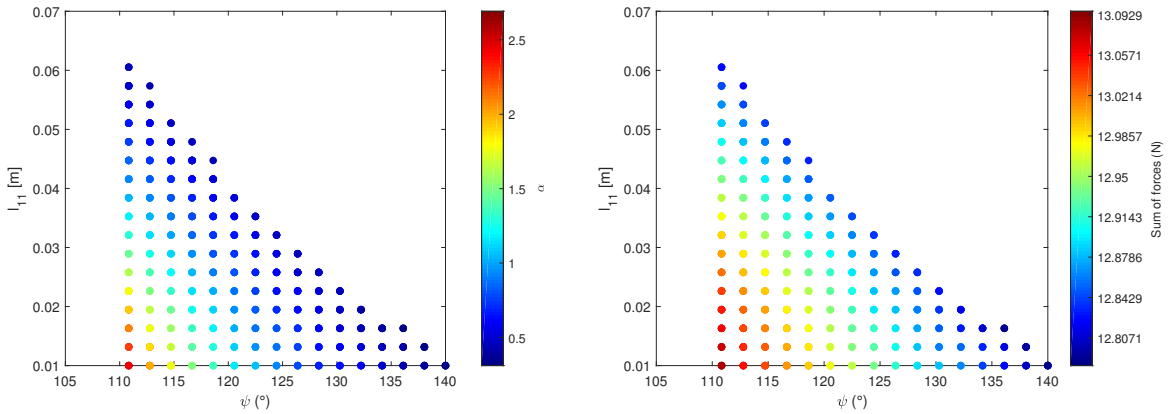

(a) Evolution of criterion α (b) Evolution of the sum of normal forces

Figure 4.8: Study of the force repartition for the variation of the parameters l_{11} l_{22} and psi

The same results are obtained with a high value of l_{11} and low value of ψ. A linear relation between those two parameters has then be used in the previous section for the analysis of other parameter.

Then when analysing the value of both criteria, we see that the two criteria go against each other. The value of α is minimised for high value of l_{11} whereas the sum of forces are maximised for the low value of it. The amplitude of variation of the sum of forces is but very low. Only a $0.2N$ variation appears. The variation of the parameter α is by opposition quite important. That is why, we finally will try to maximise the value of ψ for a given l_{11}. Finally one variable remain, l_{11} for the dynamic analysis. The ratio r was chosen from the singularity removal and force closure. The variable ψ is maximised. The relation given on equation (4.15) was used for the static analysis with p the ratio giving l_{11} from l_{21}. It gives here the upper line equation in dark blue with here $l_{21} = 0.0494m$.

$$\psi = -25.6p + 140° \tag{4.15}$$

Study of the influence of parameter l_{21}, l_{11} and l_{22} On figure 4.9, the variation of parameter l_{21} is added, the value of ψ being function of both l_{21} and p.

The transmission ratio r has still nearly no influence on the forces. The ratio p has a low influence too. It validates the choice of the parameter ψ which maximise the value of α. It stays no the influence of the length l_{21}. Once again, the sum of forces is maximised when the criteria α is maximised. They are in opposition. The parameter α is nearly null, leading to an isotropic finger when l_{21} is around $0.04m$. The sum of the forces are but not maximised. The forces will be increased when l_{21} is maximised. This figure must be moreover be put in regard to the previous figure 4.6. The design will be more robust if the finger is not isotropic. By opposition, if the object is in the center position, the optimal value of l_{21} for isotropy is a bit lower.

Study of the influence of parameter l_{21}, b and l_{hand} In this section the influence of the length of the hand and of the palm is again studied and the results of the analyse of forces is presented on figure 4.10. The length l_{hand} had an influence on criteria α but no influence on the sum of forces. That is why, only b and l_{21} are varying on figure 4.10b. The results are this time decorrelated between figure 4.10a and 4.10b.

The first analyse is down on figure 4.10a. On this figure, we see that a quasi isotropic finger can be obtained for any value of l_{hand} if the value of l_{21} and b are well chosen. It appears that

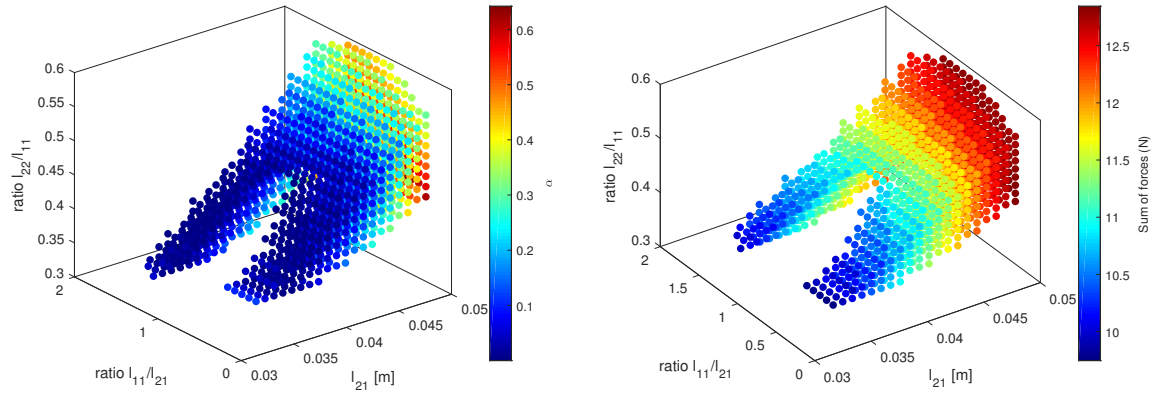

(a) Evolution of criterion α (b) Evolution of the sum of normal forces

Figure 4.9: Study of the force repartition for the variation of the parameters l_{11} l_{22} and l_{21}

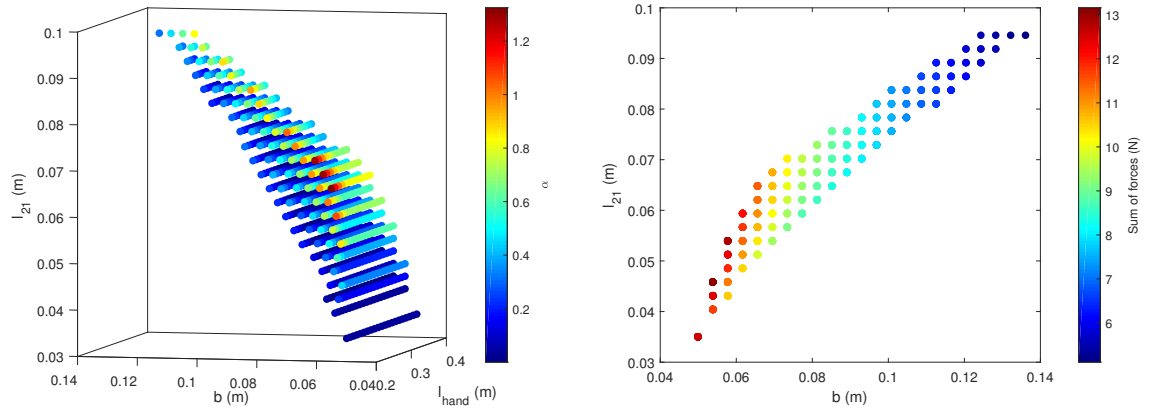

(a) Evolution of criterion α (b) Evolution of the sum of normal forces

Figure 4.10: Study of the force repartition for the variation of the parameters b l_{21} and l_{hand}

a relation, seaming linear exist between l_{21} and b leading to a quasi isotropic area when b is maximised, l_{21} being fixed. When b is decreased for a given value of l_{21}, the criteria α increases. Similarly, low value of l_{hand} when b is low leads to an increasing value of α.

When looking at figure 4.10b, we see the results are completely different. The variation with parameter b in particular is different. Low value of b leads to high values of forces and high value of l_{21} leads to higher forces.

In order to improve both criteria, the value of b must be minimised and then, a compromise between high forces and low α must be chosen as said on the previous paragraph.

Once again a lower parameter α goes in contradiction with the form closure criteria and sum of forces.

4.3 Dynamic analysis

The dynamic analysis of the gripper has two main objectives. The first objective is to design the gripper. In order to design a gripper a criteria must be chosen. It has been chosen to analyse the effect of the design on the time to convergence and on the energy given to the cylinder. Moreover, the design leading to the crossing of the maximum energy value or leading to the loss of static equilibrium of the cylinder are discarded. The second objective is to know, having a given object to catch, if the gripper is able to grasp it, and therefore which torque

must be applied and where to catch the object.

4.3.1 Solver choice

In order to simulate the closure of the hand, the choice of the solver was very important. Indeed, the contact model leads to very high stiffness in the model. To be able to simulate this, a variable step solver had to be chosen. Moreover it was necessary to chose a stiff solver, meaning it is able to deal with high non linearities. That is why the solver 'Trapezoidal Rule with the second order Backward Difference Formula' (TR-BDF2) was chosen. Moreover the zero crossing detection is used to be able to detect the appearance of different contact, using the crossing of variable δ. The detection of singularities in case they appear is also checked with the zero crossing detection. Similarly, the zero crossing of generalised joint coordinates velocities is checked to avoid during the calculation multiple zero crossing due to instability in the simulation. By using all those zero crossing detection, instability of the simulation are prevented.

4.3.2 Analysis of the simulation

Before going further, it is important to understand what is the behaviour of the gripper according to the time. It will then be understood why the model of contact is important, and then what are the limits of the model.

Kinematic behaviour of the gripper On figure 4.11 are represented the joint generalised coordinates evolution according to the time.

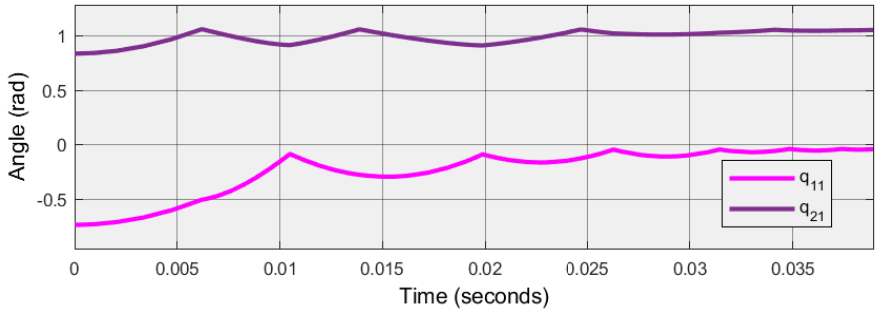

Figure 4.11: Evolution of q_{11} and q_{21} according to the time

Chronologically, the proximal phalanx hits the object. A first rebound appears visible on angle q_{21}. Then the distal phalanx continues to go toward objects and touches the object. The rebound is this time visible on joint q_{11} signal. Due to losses on each contact, the amplitude of each of the joint coordinates converge toward a final value. This is the static pose of the finger. Between each of the impacts, no forces are exerted between the object and the finger. Only the impact forces appears.

A last remark is that the torque does not influence the type of instability appearing. In particular the height of bounces is nearly not influenced by the torque. This result does not seem logical at first sight but this is because the friction in the joints were neglected. That is why the design is not very much influenced by the torque. It has been chosen to chose a first value of the torque which is half to the initial optimal value for the torque. This way the design is quite free, but the condition of instability could appear if the design is not well chosen. The chosen torque is $0.5Nm$.

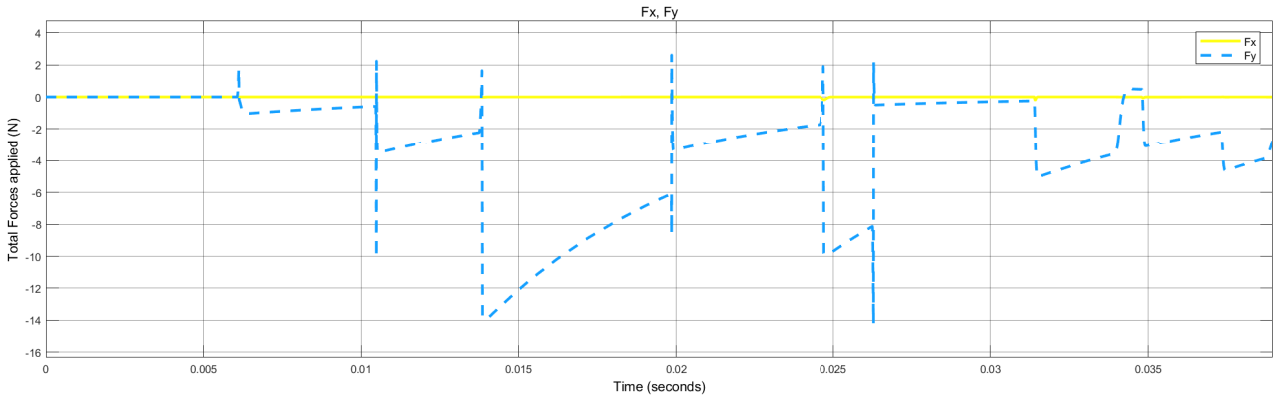

Figure 4.12: Evolution of q_{11} and q_{21} according to the time

Resultant force on the object By finding the resultant on the object of all impact forces, the forces along **x** and **y** are obtained on the object. By applying a low pass filter, the forces equivalent to the case no bounce would appear are obtained. The figure 4.12 show the evolution of the calculated forces according to the time.

It appears on this figure that the forces along **x** are null. This is due to the symmetry. The forces along y are negative, directed towards the palm. This is due to both the friction on the phalanx, keeping the object in the hand, and due to the impact exerted by distal phalanx. When impacts occurs, peak force leads to positive forces. The impact criteria can give the possibility to stop the simulations if the impact are to important. This graph has but no real physical meaning due to the filtering and because only impacts occurs. That is why the criteria of forces is not efficient if impacts occurs and the result of the forces criteria must be taken with caution. Moreover, that is an other reason why, in the dynamic analysis, the two fingers are initially symmetric, leading to less impact of this criteria on the simulation stopping. Only when forces convergences, at the end of the simulation, this criteria is here important. But this case has already been taken into account.

4.3.3 Analysis of dynamic stability

In this part, the analysis of the design parameters and their effect is studied. The torque chosen is $0.5Nm$. This torque has been chosen because it high enough to lead both on stability or instability depending on the design.

Effect of parameter l_{11}

The first analysis is done on the parameter l_{11}. The parameters ψ and l_{22} are chosen accordingly as explained in the static analysis. l_{11} has a low impact on the static results. It has then been chosen to study it in dynamic to show it now matters. The results are presented on figure 4.13.

The evolution of the energy given to the cylinder after impact according to l_{11} visible on figure 4.13a is logical. As the variable l_{11} increase, the inertia of the hand raise. That is why the impact energy raise. The maximum value of energy are moreover presented. They correspond respectively for the maximum rotational energy and for the maximum translational energy, to a maximum angle for the cylinder of $1°$ and a maximum displacement of $1mm$.

It finally appears that the maximum value for l_{11} given b, l_{21} and l_{hand} is here $7.2cm$. The best value for this parameter is but the lowest value possible, which is due to technological limits.

Moreover, the evolution of time according to l_{11} on figure 4.13b is much more chaotic. The value beyond the stable area are not relevant because the simulation was stopped before the

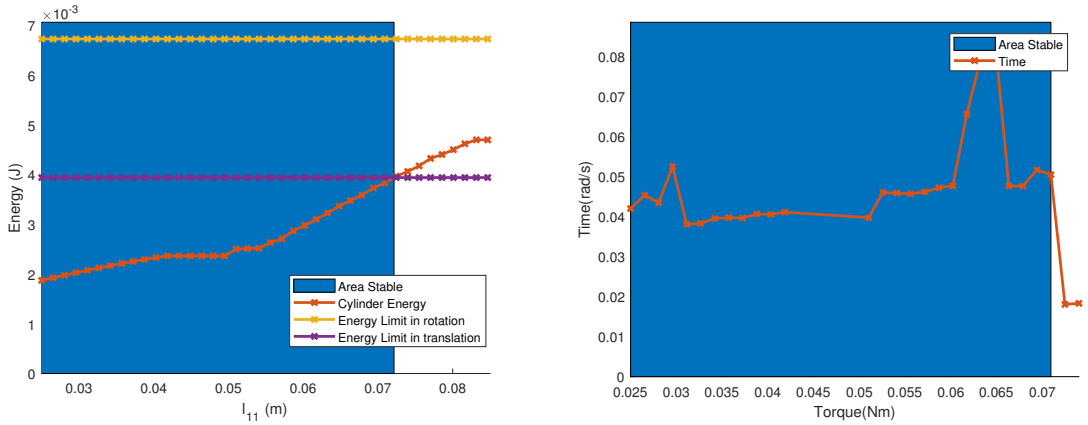

(a) Evolution of the first impact energy in function of l_{11}

(b) Evolution of the simulation time in function of l_{11}

Figure 4.13: Effect of l_{11} on the dynamic behaviour

stability. The fact it is chaotic is due to the bounce. The way the finger bounces on the object depends of the shape of the finger. Here for a value of $l_{11} = 0.062$, the finger takes nearly twice the time it takes for a value of $l_{11} = 0.067$. It appears but that some design can lead to a better robustness in relation with times. Particularly between $l_{11} = 0.032$ and $l_{11} = 0.05$, the time to convergence is quasi constant and is equal to $0.04s$. Those instability of the simulation time according to the design must be kept in mind for the rest of the analysis.

Coupled effect of parameter l_{hand},b and l_{21}

The parameters L_{hand},b and l_{21} are more complex to chose according to the static results. The analysis is continued in dynamics. On figure 4.14 is represented the area of dynamic stability according to the previous parameters. The other parameters, l_{11}, ψ and l_{22} are chosen similarly as it was done in static.

Three areas are represented. The simulation in dynamics has indeed been carried out where the static criteria were already resolved. The three areas correspond to the stability, the instability due to the criteria of forces, the instability due to the criteria of impact.

The stability is found for the low value of l_{hand}, with b and l_{21} being fixed. This means that the distal phalanges must not be to long. Indeed if the distal length are to long, the impact on distal phalanges are bigger, which leads to high bounces. The simulation becomes slightly different for both the fingers and a force is applied on the cylinder along $\mathbf{x}$. The cylinder is destabilized and has a risk to go away of the grasp.

Three yellow points appears, corresponding to high impact on the proximal phalanges. They appear for high value for both l_{21} and l_{hand}, b being quite small. The finger is just bigger, leading to higher inertia, the impact are higher.

Four points shows that the simulation and criteria are not yet perfect. Indeed, for $b = 0.06$ with $l_{hand} > 0.35$, two first points with very high value of l_{hand} leads to the stability. The simulation leads here to a perfect symmetry, the force criteria is verified. An index showing that those two designs are not good, is that the convergence time is $0.11s$ which is very long compared to other designs, as shown on figure 4.15a. That is why those designs have been discarded. Moreover, the two other surprising results are found for $b = 0.08$ and low value of l_{hand}. Those two designs leads to instability even if it seems clearly that they are in the stable area. To conclude this part, the filtering of the force may not be perfect and a very low offset will lead to an instability. It has been chosen to suppose the hand is centred during the dynamic analysis because it is supposed that if the cylinder is pushed along $\mathbf{x}$, the other

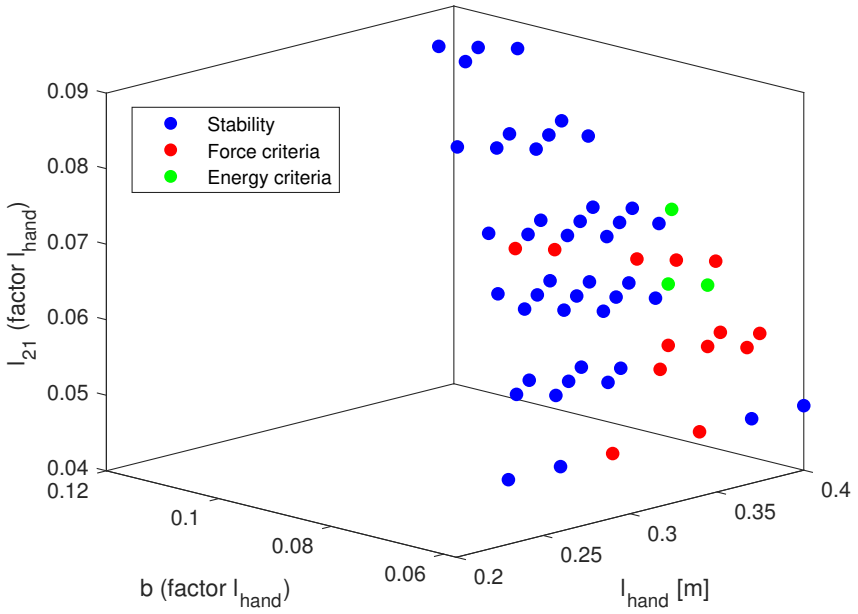

Figure 4.14: Stable and unstable area for the variation of parameter l_{hand},b and l_{21}

finger will anyway be opposed to this movement. Moreover if there is an offset, the hand will always have a tendency to bring back the object toward the center which seems interesting. The experimental analysis will here be necessary to validate this result.

Definition of an objective function The question, now we know where the hand can lead to the stability is how can we choose the design among the solutions. Two criteria are analysed. On figure 4.15a, the time to convergence is plotted, on figure 4.15b, the proximal impact energy given to the cylinder is plotted. The convergence time is calculated only for the design leading to stability, the impact energy can be calculated in any case.

Evolution of time to stability The evolution of time according to the design parameter is very understandable. The diminution of the size of the hand leads to a faster convergence. The minimum time of convergence is $0.04s$ and appears for the smaller possible designs. If we take the all the smallest value of l_{hand}, b and l_{21} varying, we can observe that low value of convergence time can be found too. The increase of l_{21} leads but to the increase of the convergence time.

Evolution of cylinder energy The evolution of energy given to the cylinder on figure 4.15b is harder to interpret. A general idea is but first that the increase of l_{hand}, b and l_{21} being fixed, corresponding to the increase of t_{22}, makes the impact energy smaller. This means that the energy after impact is transmitted to the distal phalanges. The impact done by distal phalanges are bigger. The impact energy on the proximal phalanges is then not a sufficient criteria for stability because the impact on distal phalanges seems too to destabilize the object.

Conclusion The impact energy should then be used more as a constraint than an objective in the design process. The filtering of the forces could be improved, the criteria but brought some interesting results anyway discarding design with long distal phalanges. This can certainly be used as a constraint too.

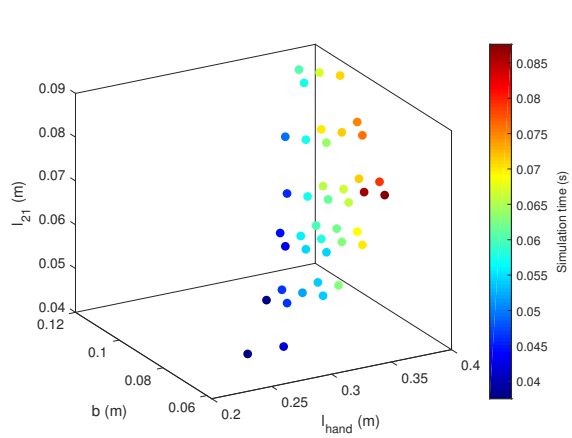

(a) Convergence time

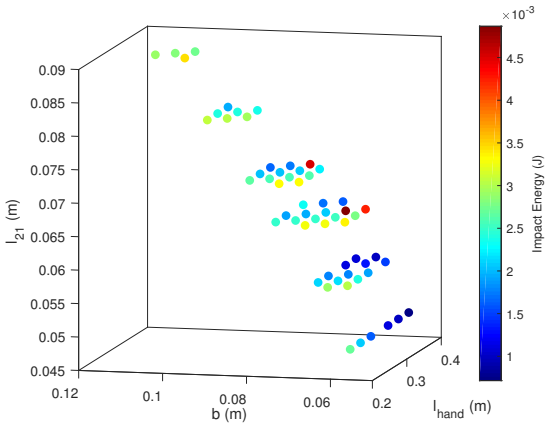

(b) Energy given to the cylinder after the first impact

Figure 4.15: Study of the dynamic design criteria in function of b l_{21} and l_{hand}

The time to convergence seems, in the contrary, very efficient as an objective for the design process. This criteria will indeed leads to a convergence toward a small hand with small inertia. It will moreover help discarding the avoidance of stability problems. This criteria is moreover very complimentary to the static criteria because it gives the optimal value for l_{hand} or quite equivalently to t_{22}, and to l_{11}. Previously those parameter had a quite low influence. By opposition, the value of l_{21} or b have a quite low influence in dynamic in comparison to the static results.

Analysis of the hand performances

The design process being now more clearer, the question is what type of object will it be possible to catch. The simulation and impact criteria can moreover answer to the question how to catch the object to prevent the object to move.

Influence of the torque The evolution of the time and cylinder energy in function of the torque is presented on figure 4.16. It must be noted that the spring constant torque is still not constant. It is proportional to the applied torque. This study is then done in order to chose the optimal torque and spring stiffness to close the hand quickly.

To begin with, a minimal torque exist, even if the spring constant is function of the torque. This case appears if the maximal torque to prevent the distal phalanx to fold to early is inferior to the minimal torque required to close the finger on the object.

The maximal torque is found either due to the impact criteria or due to the force criteria. In the design presented here, the instability comes from the impact as shown on figure 4.16b. The cylinder energy after impact is proportional to the applied torque. The maximum torque found is equal to $0.9Nm$.

On figure 4.16a, the time to stability decrease with the torque increasing. This results seems logic as the cylinder does not move, and stay true only if the cylinder keeps it stability.

Influence of the cylinder density In the case of the cylinder density, both the limits and the energy given to the cylinder evolve according to the time as shown on figure 4.17. The maximum energy is linearly related to the cylinder density. By opposition, the energy given to the cylinder is inversely proportional to the density. It is therefore very difficult to catch a light object without making it moving. With the chosen torque of $0.5Nm$, the maximum density is $730kg \cdot m^{-3}$. In order to catch a smaller object with this criteria, the torque must be reduced.

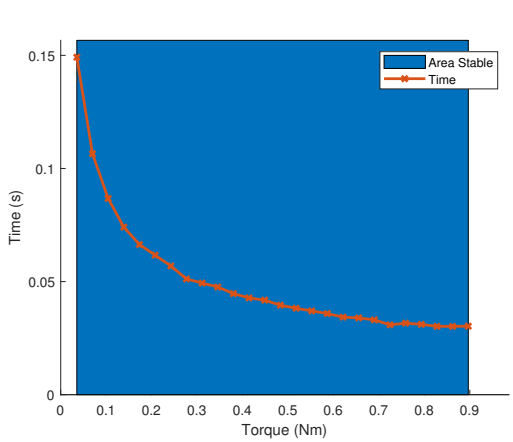

(a) Convergence time

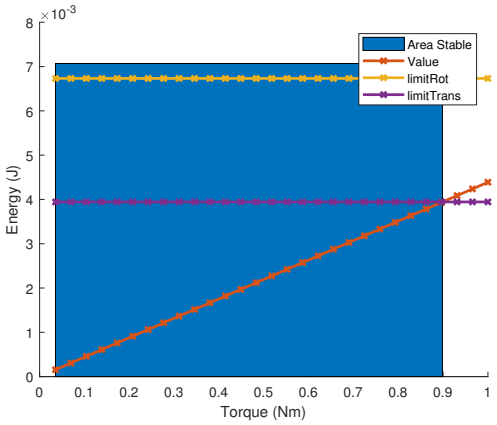

(b) Energy given to the cylinder after the first impact

Figure 4.16: Study of the influence of the torque on the stability and on the convergence time

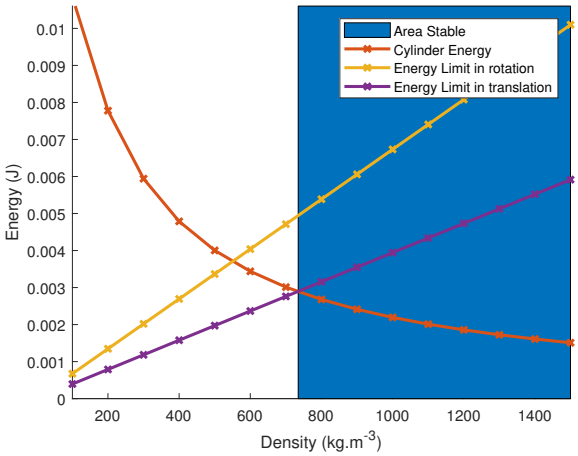

Figure 4.17: Influence of the cylinder density on the cylinder stability

Influence of the height of grasping Last but not least, the height of grasping influences the stability of the cylinder. It does not influence the convergence time. On figure 4.18, the energy of the cylinder is plotted in function of the height the object is grasped.

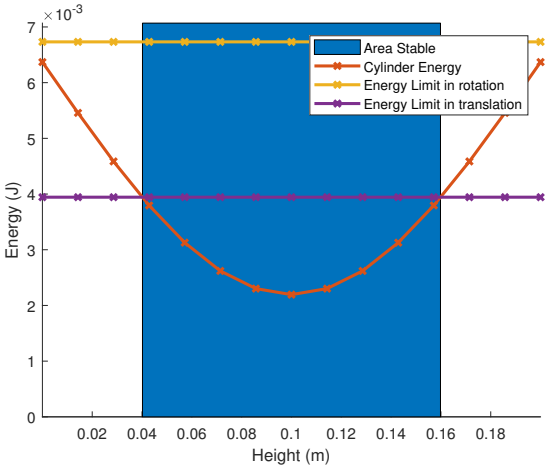

Figure 4.18: Influence of the height of the grasping on the cylinder stability

The cylinder is destabilised in two cases, if it is taken to low or to high. The stability is better around the middle. In this case the energy given to the cylinder is minimal on the middle. It must be here reminded that this criteria is valid only for the impact. The energy is given nearly instantaneously to the object, the friction on the ground bring is neglected during the impact. But if no impact occurs, it is better to grasp the object lower, preventing to give a moment through the gripper and the ground. This conditions should be tested experimentally.

4.4 Proposed methodology of design

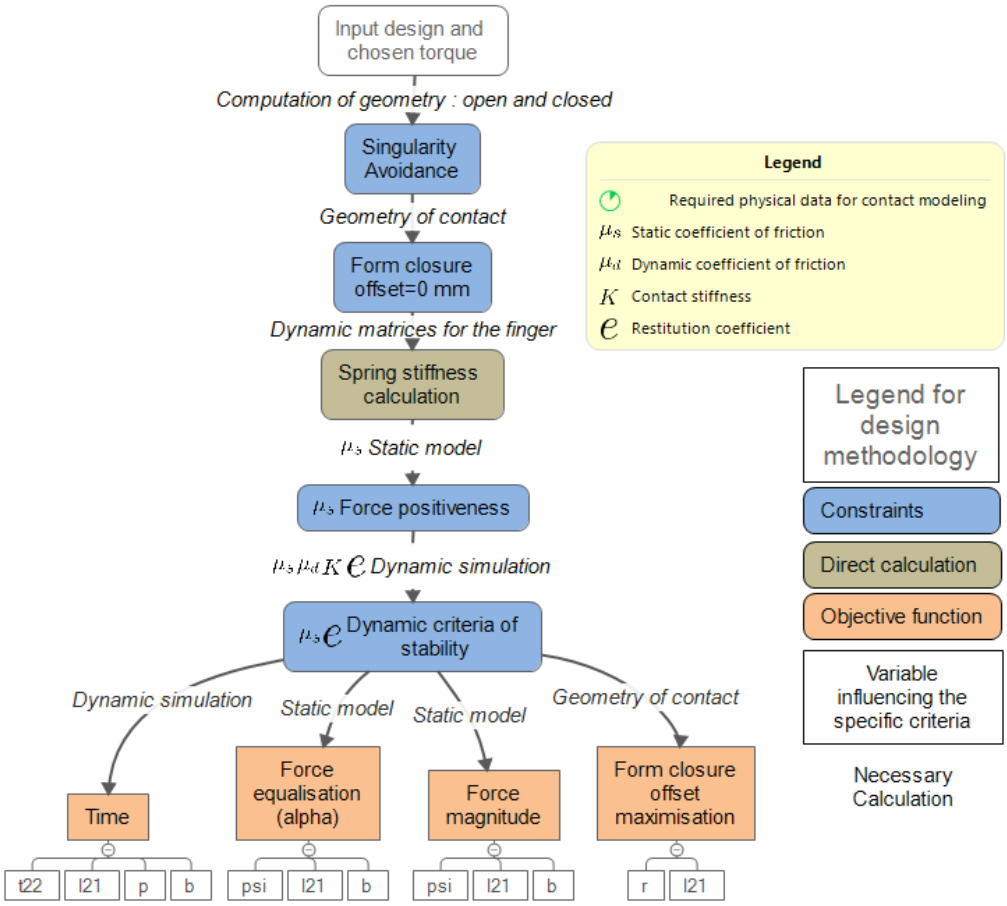

Figure 4.19: Proposed methodology for the design of a gripper

According to the design analysis done in the previous section, a design methodology is proposed here. The figure 4.19 present the general idea for the design of the gripper. The first step is to chose a torque adapted for the object. This can be done by running several simulation with a design checking all geometric and kinematics constraints. The torque can then be chosen, being inferior to the maximum torque.

The optimisation can then start. The optimisation variable chosen for the design are the lengths l_{21}, b, t_{22}, the ratios r and p, the angle ψ. Five constraints must be checked. Four objective functions have been defined. The objective functions could be normalised and use them in combinations to define an objective function. An other solutions consist in trying to find pareto-optimal solutions with the four objective functions or less.

All objective functions cannot be evaluated if some of the constraints are not checked. It make no sense for example to evaluate the form closure if the given configuration cannot be

reached. At this point the object could be moved with the $offset$. The maximum offset for which the form closure is checked is the first objective function.

Then the static model can be evaluated, the spring stiffness can be calculated, the constraint of force positiveness and palm force positiveness can be calculated. At this point the two objectives for the force equalisation (minimisation of α) and the maximisation of the force magnitude can be computed.

Once all the previous constraints are checked, the simulation of the dynamic model of the hand can be launched. Two constraints which are the impact criteria and the force criteria to evaluate the object stability are verified. Finally, if the constraint are checked, the last objective which is the convergence time can be computed.

If any of the constraint is not checked, the design has to be discarded, some of the objective could be evaluated but not all.

Conclusion

4.5 General conclusion

During the master thesis, the objective was to provide a new methodology to design a gripper with its dynamic. The first important part was the modelling. Different issues appeared for that. First the static model had to be carried out. The dynamic model of the system was then studied. To evaluate the contact forces, the kinematic of contact was implemented. The study of existing contact model was then carried out during the master thesis. The implementation and checking of the model with a cross relation with Adams have then been done.

A study has then been performed to define new dynamic criteria of stability. The theory of contact lead first on a first criterion. In particular the energy given by the finger to the cylinder was calculated and used to define new criteria of stability. Then a dynamic criteria is defined to check that the object is statically equilibrate when the fingers are in contact with the cylinder. Those two criteria are used after in the dynamic analysis.

The next step consisted in the study of the results. The choice of studied parameters was done in order to simplify the future analysis in dynamic. A new method to define the spring is given according to the dynamic model of the finger. The analyse of the kinematics of the finger and of the static stability of the finger was then achieved. The conclusion leads to the choice of most of the parameter of the finger. The choice of the last parameters and of the torque is possible thanks to the dynamic results. The study of the dynamics of the finger was able to tell which type of object the gripper can catch and at which speed. Finally thanks to this analysis, a design methodology is proposed.

4.6 Extension and improvements

The design of the gripper according to the kinematics, the static and the dynamic can now be implemented. The optimisation process should be able to find specific designs. An experimental work is moreover planned. It will give the possibility to validate the new design and to validate the design process. In particular the correlation between the defined criteria of stability and the actual study on a prototype will be important.

Appendix A

Complimentary calculations

A.1 Cylinder kinematic

The first step to compute the dynamic of the cylinder is to compute the kinematics relations. The kinematic of the cylinder is defined with the coordinates of the center of gravity and with three angles. It is necessary to compute the rotational velocity of the cylinder. This vector defines the rotation axis and the norm of the resultant rotational velocity.

If we use the Euler angle with the rotation z,x,z, the relation is given as follow:

$$\boldsymbol{\omega} = \mathbf{M}_{\omega\mathbf{2a}} \begin{bmatrix} \dot{\psi} \\ \dot{\theta} \\ \dot{\phi} \end{bmatrix} \tag{A.1}$$

With :

$$\mathbf{M}_{\omega\mathbf{2a}} = \begin{bmatrix} 0 & \cos\psi & \sin\psi\sin\theta \\ 0 & \sin\psi & -\cos\psi\sin\theta \\ 1 & 0 & \cos\theta \end{bmatrix} \tag{A.2}$$

With this first relation, it is possible to get $\boldsymbol{\omega}$ from the Euler angle. Omega is a necessary vector in the dynamic model. Then the dynamic model will give $\dot{\boldsymbol{\omega}}$. To get then the accelerations of angle, the following relation is used :

$$\begin{bmatrix} \ddot{\psi} \\ \ddot{\theta} \\ \ddot{\phi} \end{bmatrix} = {\mathbf{M}_{\omega\mathbf{2a}}}^{-1}\dot{\boldsymbol{\omega}} - \begin{bmatrix} \cos\theta & 0 & -1 \\ 0 & \sin\theta & 0 \\ -1 & 0 & \cos\theta \end{bmatrix} \begin{bmatrix} \frac{\dot{\psi}\dot{\theta}}{\sin\theta} \\ \dot{\psi}\dot{\phi} \\ \frac{\dot{\phi}\dot{\theta}}{\sin\theta} \end{bmatrix} \tag{A.3}$$

Once all the parameters are expressed, it is possible to define the direction vector of the cylinder :

$$\mathbf{z_c} = {}^{\mathbf{0}}\mathbf{R_3} \begin{bmatrix} 0 \\ 0 \\ 1 \end{bmatrix} \tag{A.4}$$

And its derivative :

$$\dot{\mathbf{z_c}} = \begin{bmatrix} \cos\psi\sin\theta & \sin\psi\cos\theta \\ \sin\psi\sin\theta & -\cos\psi\cos\theta \\ 0 & -\sin\theta \end{bmatrix} \begin{bmatrix} \dot{\psi} \\ \dot{\theta} \end{bmatrix} \tag{A.5}$$

A.2 Cylinder Dynamic

Then the dynamic equation can be expressed with the following equations :

$$\ddot{\mathbf{X}} = \frac{1}{m_{cyl}}\mathbf{F} \tag{A.6}$$

$${}^{0}\dot{\boldsymbol{\omega}}_{\boldsymbol{c}} = {}^{0}\mathbf{R_3}\mathbf{I_{cyl}}^{-1}\left({}^{0}\mathbf{R_3}^{T}\mathbf{M} - {}^{3}\hat{\boldsymbol{\omega}}_{\boldsymbol{c}}\mathbf{I_{cyl}}{}^{3}\boldsymbol{\omega}_{\boldsymbol{c}}\right); \tag{A.7}$$

With :

$${}^{3}\boldsymbol{\omega}_{\boldsymbol{c}} = {}^{0}\mathbf{R}_{3}^{T}{}^{0}\boldsymbol{\omega}_{\boldsymbol{c}} \tag{A.8}$$

A.3 Contact in three dimensions

In the case the contact is not in the plane of the hand, the normal of contact $\mathbf{y}_{ci}$ is different from the normal of the phalanx $\pm y_{2i}$. The forces computed on equation (2.70) and (1.15) must be projected.

A.3.1 Tip contact modelling

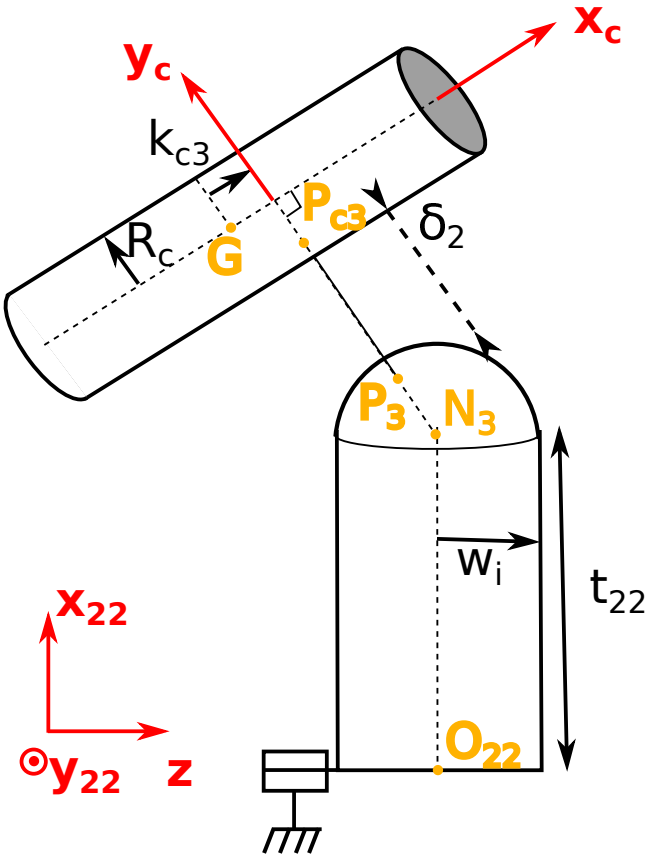

Figure A.1: Tip contact modelling

The tip contact is modelled similarly as in part 2.4.2. The figure A.1 shows the geometry in case the contact is done with the tip of the finger. The tip is modelled with a sphere of radius w_i. The procedure to evaluate the pentration depth, penetration depth velocity and slip velocity is similar but take this time as reference the distance between the axis of the cylinder and the center of the tip.

The first step consist in evaluating the the relative position between the center of the tip N_3 and the center of mass of the object G.

$$\overrightarrow{\mathbf{GN}_3} = \overrightarrow{\mathbf{OO}_{22}} + t_{22}\mathbf{x}_{22} - \mathbf{X}_G \tag{A.9}$$

The length of contact k_{c3} of the cylinder is directly evaluated by a projection on $\mathbf{x}_c$.

$$k_{c3} = \overrightarrow{\mathbf{GN}_3} \cdot \mathbf{x}_c \tag{A.10}$$

The projection of point N_3 on the axis of the cylinder can then be obtained.

$$\overrightarrow{\mathbf{N}_{c3}\mathbf{N}_3} = \overrightarrow{\mathbf{GN}_3} - k_{c3}\mathbf{x}_c \tag{A.11}$$

By taking the norm, the distance d between the two objects is calculated.

$$d = \left\| \overrightarrow{\mathbf{N}_{c3}\mathbf{N}_3} \right\| \tag{A.12}$$

And the unitary vector normal to the contact is obtained.

$$\mathbf{y}_c = -\frac{\overrightarrow{\mathbf{N}_{c3}\mathbf{N}_3}}{\delta} \tag{A.13}$$

The penetration depth is evaluated by removing the thickness of the finger and of the object.

$$\delta = d - R_c - w_i \tag{A.14}$$

The relative velocity $\mathbf{V}_{rel}$ between the two points of contact can finally be obtained. First in the case the cylinder can move.

$$\mathbf{V}_{rel} = \dot{\mathbf{X}}_G + k_c\dot{\mathbf{x}}_c - t_{22}\dot{\mathbf{x}}_{22} - l_{21}\dot{\mathbf{x}}_{21} - R_c\boldsymbol{\omega}_c \times \mathbf{y}_{ci} - w(\dot{\theta}_1 + \dot{\theta}_2)\mathbf{z} \times \mathbf{y}_{ci} \tag{A.15}$$

If the cylinder does not move, the expression is more simple.

$$\mathbf{V}_{rel} = -t_{22}\dot{\mathbf{x}}_{22} - l_{21}\dot{\mathbf{x}}_{21} - w(\dot{\theta}_1 + \dot{\theta}_2)\mathbf{z} \times \mathbf{y}_{ci} \tag{A.16}$$

A.3.2 Projection on the finger

To do this, the forces are first summed as shown on equation. (A.17).

$${}^j\mathbf{F}_i = {}^j\mathbf{F}_{ni} + {}^j\mathbf{F}_{ti} \tag{A.17}$$

They are then projected on the normal and tangent vector of the finger in two dimensions, respectively $\mathbf{x}_{2i}$ and $\mathbf{y}_{2i}$, on the first or second phalanx.

Moreover a moment appears along the direction $\mathbf{z}$ normal to the finger plane. It can be expressed with relation (A.19).

$$\tau_i = (\tau_{fric}\mathbf{y}_{ci} + \overrightarrow{\mathbf{N}_i\mathbf{P}_i} \times \mathbf{F}_i)) \cdot \mathbf{z} \tag{A.18}$$

$$= \tau_{fric}\mathbf{y}_{ci} \cdot \mathbf{z} + w_i\mathbf{y}_{ci}^T \begin{pmatrix} F_{iy} \\ -F_{ix} \\ 0 \end{pmatrix} \tag{A.19}$$

Appendix B

Data

Additional results are presented in this part. A zoom is done in order to make the analysis of the parameter b l_{21} and l_{hand} easier.

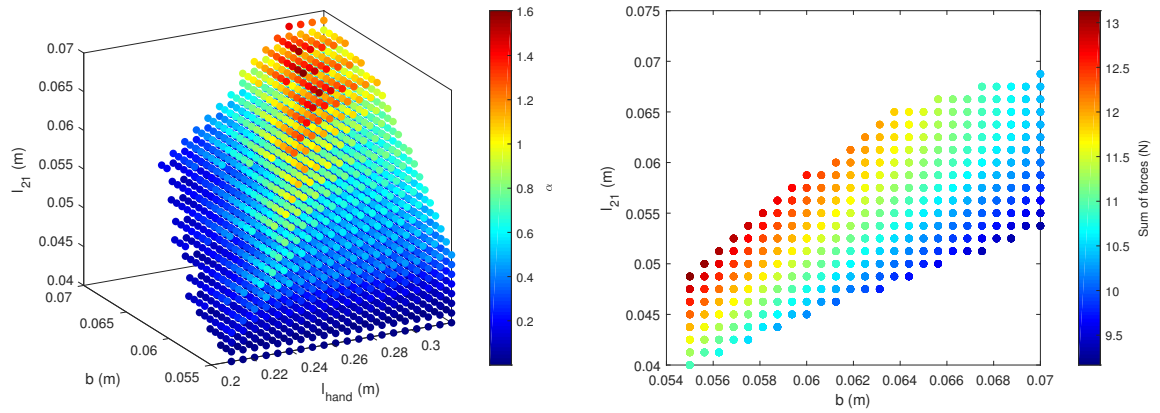

(a) Evolution of criterion α (b) Evolution of the sum of normal forces

Figure B.1: Force closure area for the variation of the parameters b l_{21} and l_{hand} with a zoom on the interesting part of the graph

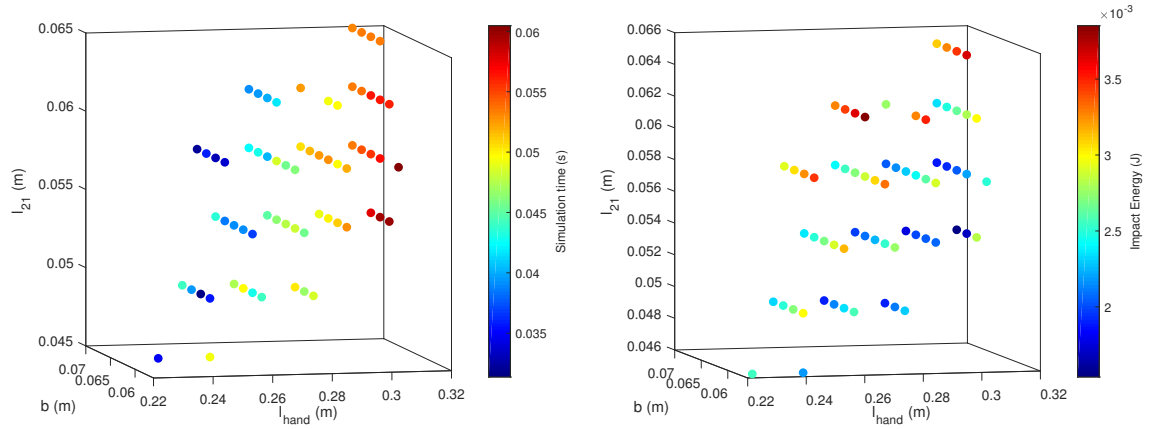

(a) Evolution of the convergence time (b) Evolution of the impact energy

Figure B.2: Dynamic analysis for the variation of the parameters b l_{21} and l_{hand} with a zoom on the interesting part of the graph

Bibliography

[1] V. Begoc, "Etude et conception d'un préhenseur versatile sous-actionné : application dans la préparation de commandes de détail," Français, Université des sciences et techniques de Montpellier 2 (1970-2014), 2008.

[2] L. Birglen, T. Laliberté, and C. Gosselin, *Underactuated robotic hands*, springer-v ed., B. Siciliano, K. Oussama, and G. Frans, Eds., 2007.

[3] S. Krut and V. Begoc, "A simple design rule for 1st order form-closure of underactuated hands," *1st International Workshop on Underactuated Grasping*, vol. 2, no. 1, pp. 1–7, 2010.

[4] R. A. Stavenuiter, L. Birglen, and J. L. Herder, "A planar underactuated grasper with adjustable compliance," *Mechanism and Machine Theory*, vol. 112, pp. 295–306, 2017. [Online]. Available: http://dx.doi.org/10.1016/j.mechmachtheory.2016.08.001

[5] M. Higashimori, S. Nishio, and M. Kaneko, "Dynamic preshaping based optimum design for high speed capturing robots," *2005 IEEE/RSJ International Conference on Intelligent Robots and Systems, IROS*, pp. 2930–2935, 2005.

[6] M. A. Saliba and C. W. De Silva, "Quasi-dynamic analysis, design optimization, and evaluation of a two-finger underactuated hand," *Mechatronics*, vol. 33, pp. 93–107, 2016. [Online]. Available: http://dx.doi.org/10.1016/j.mechatronics.2015.09.007

[7] S. Briot and W. Khalil, *Dynamics of Parallel Robots*, 1st ed., ser. 1. Springer International Publishing, 2015, vol. 35.

[8] L. Birglen and C. Gosselin, "On the force capability of underactuated fingers," *2003 IEEE International Conference on Robotics and Automation (Cat. No.03CH37422)*, vol. 1, pp. 1139–1145, 2003. [Online]. Available: http://ieeexplore.ieee.org/document/1241746/

[9] L. Birglen and C. M. Gosselin, "Kinetostatic analysis of underactuated fingers," *IEEE Transactions on Robotics and Automation*, 2004.

[10] S. Krut, V. Bégoc, E. Dombre, and F. Pierrot, "Extension of the form-closure property to underactuated hands," *IEEE Transactions on Robotics*, vol. 26, no. 5, pp. 853–866, 2010.

[11] D. LLEVAT PÀMIES, "Dynamic grasping of objects with a high-speed parallel robot Report," LS2N, Nantes, Tech. Rep., 2017.

[12] S. Krut, "A force-isotropic underactuated finger," in *Proceedings - IEEE International Conference on Robotics and Automation*, 2005.

[13] R. Rizk, S. Krut, and E. Dombre, "Grasp-stability analysis of a two-phalanx isotropic underactuated finger," *IEEE International Conference on Intelligent Robots and Systems*, pp. 3289–3294, 2007.

[14] H. Dong, E. Asadi, C. Qiu, J. Dai, and I. M. Chen, "Geometric design optimization of an under-actuated tendon-driven robotic gripper," *Robotics and Computer-Integrated Manufacturing*, vol. 50, no. September 2017, pp. 80–89, 2018.

[15] J. Schuurmans, R. Q. Van Der Linde, D. H. Plettenburg, and F. C. T. Van Der Helm, "Grasp force optimization in the design of an underactuated robotic hand," *2007 IEEE 10th International Conference on Rehabilitation Robotics, ICORR'07*, vol. 00, no. c, pp. 776–782, 2007.

[16] R. M. Murray, Z. Li, and S. S. Sastry, *A Mathematical Introduction to Robotic Manipulation*, 1994, vol. 29. [Online]. Available: http://scholar.google.com/scholar?hl=en{&}btnG=Search{&}q=intitle:A+Mathematical+Introduction+to+Robotic+Manipulation{#}0

[17] M. MacHado, P. Moreira, P. Flores, and H. M. Lankarani, "Compliant contact force models in multibody dynamics: Evolution of the Hertz contact theory," *Mechanism and Machine Theory*, vol. 53, pp. 99–121, 2012. [Online]. Available: http://dx.doi.org/10.1016/j.mechmachtheory.2012.02.010

[18] I. Kao, K. Lynch, and J. W.Burdick, "Contact modeling and manipulation," in *Handbook of Robotics*, B. Siciliano and O. Khatib, Eds. Springer-Verlag Berlin Heidelberg, 2008, pp. 647–666.

[19] P. Flores, M. MacHado, M. T. Silva, and J. M. Martins, "On the continuous contact force models for soft materials in multibody dynamics," *Multibody System Dynamics*, vol. 25, no. 3, pp. 357–375, 2011.

[20] F. Aghili and C. Y. Su, "Impact dynamics in robotic and mechatronic systems," *International Conference on Advanced Mechatronic Systems, ICAMechS*, vol. 2017-Decem, pp. 163–167, 2018.